Assessment of the 18 September 2011 M_W 6.9 Sikkim earthquake using very high resolution satellite data

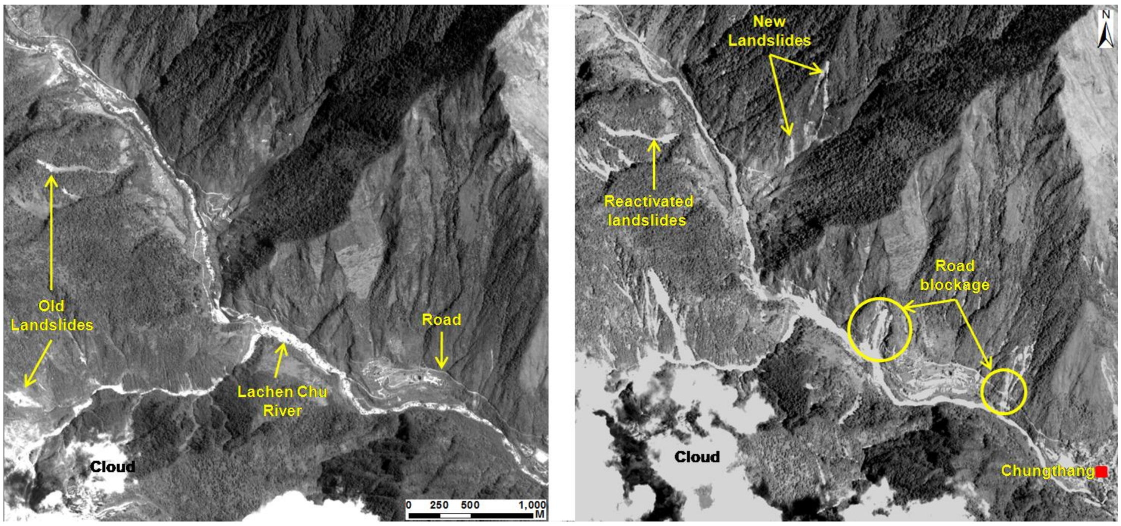

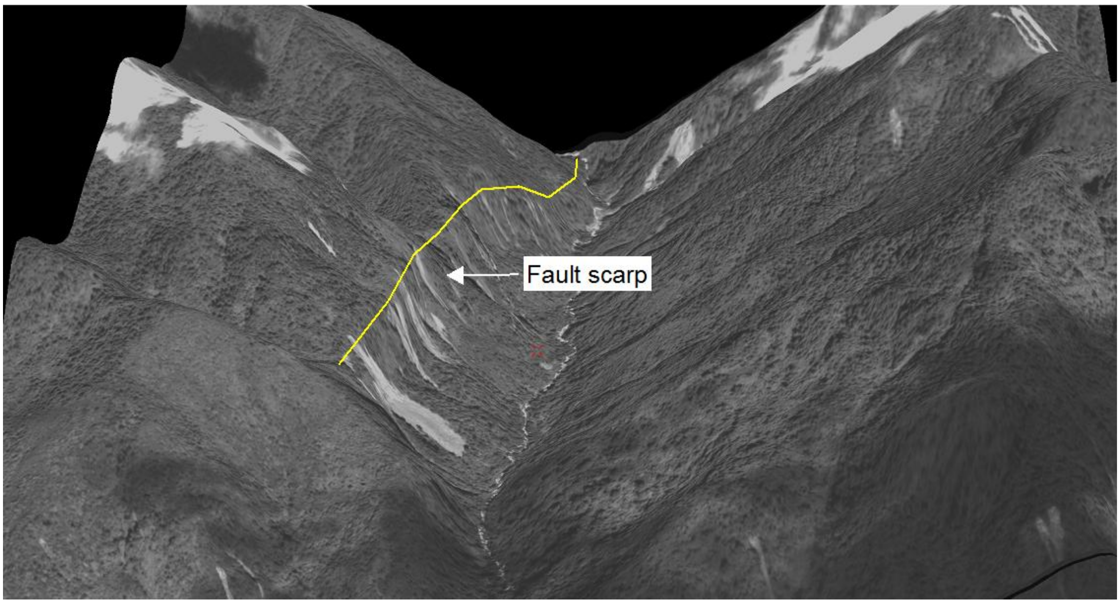

Disaster Management Support Programme

Geosciences Division
RS&GIS Applications Area
National Remote Sensing Centre
Indian Space Research Organisation
Department of Space, Govt. of India
Balanagar, Hyderabad - 500 625

NATIONAL REMOTE SENSING CENTRE

REPORT / DOCUMENT CONTROL SHEET

1	**Security Classification**	Unrestricted			
2	**Distribution**	ISRO and collaborating organisations			
3	**Report / Document version**	**(a) Issue no. 01**	**(b) Revision & Date**	**18.10.2011**	
4	**Report / Document Type**	Project report			
5	**Document Control Number**	NRSC-RS&GISAA-ERG-GD-DEC11-TR338			
6	**Title**	Assessment of the 18 September 2011 M_w 6.9 Sikkim earthquake using very high resolution satellite data			
7	**Particulars of collation**	**Pages** 34	**Figures** 11	**Tables** 1	**References** 22
8	**Author(s)**	Dr. K. Vinod Kumar, Dr. Tapas Ranjan Martha and Shri K. Babu Govindharaj			
9	**Affiliation of authors**	Geosciences Division, RS&GIS-AA, NRSC			
10	**Scrutiny mechanism**	**Compiled by** Dr. T. R. Martha	**Reviewed by** Head, Geosciences	**Approved/Controlled by** DD (RS&GIS-AA)	
11	**Originating unit**	NRSC			
12	**Sponsor(s)/ Name and Address**	ISRO			
13	**Date of Initiation**	18 - September - 2011			
14	**Date of Publication**	18 - October - 2011			

15

Abstract (with Keywords): In this report, we studied the M_w 6.9 earthquake in Sikkim, India occurred on 18 September 2011 using Cartosat-1 & 2, GeoEye-1, QuickBird-2 and WorldView-2 data, which were acquired by ISRO and USGS under the initiative of International Charter Space and Major Disasters. Total 123 image scenes from eight satellites covering an area of 4105 km^2 were analysed, 1196 new landslides were mapped, blocked roads were identified and affected villages were located. Geological assessment of the earthquake highlighted linear disposition of landslides along existing faults suggesting their reactivation.

Keywords: International Charter, Damage, Landslide, Fault, VHR, Disaster

Summary

Satellite data are known for their capability to provide firsthand information for a large area after disasters. Availability of very high resolution (VHR) satellite data immediately after a disaster has enhanced the role of remote sensing in damage assessment. In this report, we studied the M_w 6.9 earthquake in Sikkim, India occurred on 18 September 2011 using Cartosat-1&2, GeoEye-1, QuickBird-2 and WorldView-2 data, which were acquired by ISRO and USGS under the initiative of International Charter Space and Major Disasters. The earthquake affected area being in inaccessible Himalayan mountainous terrain, VHR data from these satellites provided an opportunity to quickly view the terrain both spatially and temporally. Using visual change analysis technique through comparison of pre- and post-earthquake images, we assessed the damage caused by the event. A total of 123 image scenes from eight satellites covering an area of 4105 km^2 were analysed, 1196 new landslides were mapped, blocked roads were identified and affected villages were located. Geological assessment of the earthquake highlighted linear disposition of landslides along existing faults suggesting their reactivation. The landslide inventory map prepared from VHR images also showed a good match with the earthquake shake map of USGS. Results showed several parts of north Sikkim, particularly Mangan and Chungthang, close to the epicentre, were severely affected by the earthquake.

Acknowledgements

This work was carried out under the Decision Support Centre (DSC) activities of NRSC. The guidance by Dr. V. K. Dadhwal, Director, NRSC, Dr. P.G. Diwakar, Director, EOS and Shri G. Behera, Deputy Director, RS&GIS-AA, NRSC is duly acknowledged. We thank International Charter on Space and Major Disasters for providing very high resolution satellite data for assessment of the earthquake affected area against the Charter call 372 (Earthquake in northeast India). We also thank Rynn M. Lamb, disaster response coordinator, USGS and Dr. N. Aparna, NRSC and Dr. R Nagaraja, Head, NDC for quick dissemination of satellite data for analysis purpose.

Table of Contents

1. Introduction

The Himalayas is known for active seismicity due to its tectonic setting. Regions around the Himalayas are always in the danger of earthquakes. Recently an earthquake of M_w 6.9 struck India-Nepal border on 18 September 2011 at 06:10:48 PM (IST) with its epicentre at 27.723°N and 88.064°E, and focus at 19.7 km depth (Source: USGS). The energy released by this shallow focus earthquake shook far away regions lying in the plain areas as tremors were felt in many parts of Sikkim, West Bengal, Bihar, Jharkhand, Uttar Pradesh, Delhi in India. Adjoining areas in Nepal and China also felt the tremor due to this event. As per the news reports several houses were damaged, 116 people were killed and many important roads were blocked due to landslides in Sikkim.

In recent times, disaster support activities, especially in post-disaster situations, are becoming dependent on the results derived from satellite data analysis (Tralli et al., 2005; Voigt et al., 2007). This is primarily due to the availability of large number Earth Observation satellites, and better coordination among space faring nations to share data in emergency scenarios. ISRO as a part of its disaster management support activities has programmed its satellites to acquire data over Sikkim area immediately after the earthquake. At the same time International Charter on Space and Major Disasters (ICSMD) was activated (Charter call 372) to acquire data from other satellites over the earthquake affected region.

Use of high resolution satellite data for rapid earthquake damage assessment has been shown comprehensively for three recent major earthquakes i.e. Bam, Iran; Kashmir, India and Pakistan; and Wenchuan, China (Arciniegas et al., 2007; Dunning et al., 2007; Gamba et al., 2007; Ray et al., 2009; Vinod Kumar et al., 2006; Wang et al., 2009). Vinod Kumar et al. (2006) have shown how stereoscopic Cartosat-1 data were useful for damage assessment in the 2005 Kashmir earthquake. Voigt et al. (2007) stressed that since time is a constraint and fast extraction of damage maps are desirable after a disaster situation, sophisticated image processing techniques such as atmospheric corrections should only be used if it is absolutely necessary. However, damage maps should have high planimetric accuracy for which orthorectification of satellite images should be attempted.

Apart from damage to houses, properties and infrastructures, earthquakes also trigger landslides (Di et al., 2010; Jibson et al., 2006). Several studies have shown the effectiveness of satellite data to identify landslides triggered by earthquake (Gorum et al., 2011; Metternicht et al., 2005; Stumpf and Kerle, 2011; Wang et al., 2009). Earthquake induced landslides are more dangerous in comparison to rainfall triggered landslides since the former creates mostly large deep-seated landslides capable of severe destruction. Large landslides are also capable of creating temporary dams, which may create a situation potential for flash floods (Dunning et al., 2007).

The main objective of this study is to carry out a rapid assessment of the earthquake affected Sikkim area using VHR data so that maps can be disseminated rapidly to support disaster management activities. The assessment was mainly focussed on identifying damage to roads, infrastructures, and demarcating landslides triggered after the earthquake. A geological assessment of the event was also made to find out any possible reactivation of faults in this tectonically active area.

2. Study area

Parts of Sikkim, India covering an area of 4105 km^2 were analysed for damage assessment (Fig.1). This area is in the high Himalayan terrain, where occurrence of earthquakes and landslides are frequent (Ghosh et al., 2010; Kayal, 2001). Gangtok, the capital of Sikkim state, is a major city in this area. Kanchenjunga (8586 m), the third highest mountain peak of the world is located in the study area. Major parts of the north Sikkim are covered by snow and glaciers, which are the sources to many perennial rivers in the Indo-Gangetic plain. Tista is the major river in this area and is a tributary to the Brahmaputra river.

2.1. Geological setting

Geologically, Sikkim Himalayas is a seismically active area as the Indian plate is subducting under the Eurasian plate at approximately 50 mm/yr. The zones of subduction are represented on the surface in the form of main boundary thrust (MBT) and main central thrust (MCT). While MBT separates low grade lesser Himalayan rocks in the north from Siwalik group of rocks in the south, MCT separates high grade central crystalline rocks in the north from low grade lesser Himalayan rocks in the south. MCT and MBT are the two major tectonic features in the Sikkim Himalayas around which most of the earthquake epicentres were located. Last time this area experienced a major earthquake (M_w 5.3) was on 14 February 2006 (Raju et al., 2007).

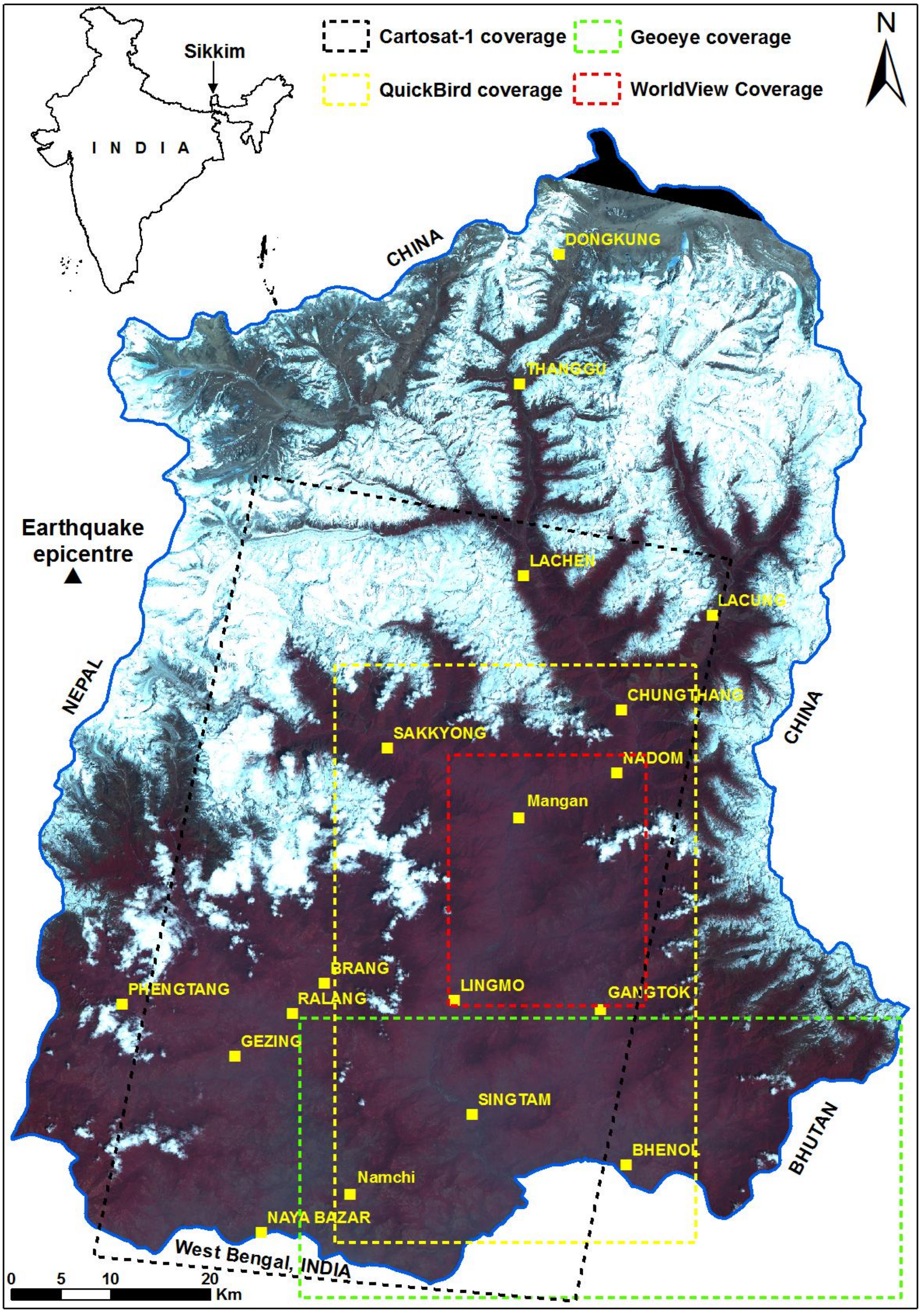

Fig. 1. Synoptic view of Sikkim showing post-earthquake VHR data coverage.

3. Data sources

To assess damage caused by the earthquake, ISRO has programmed its satellites to acquire VHR and microwave images of Sikkim immediately after the event. Subsequently, on 19 September 2011, data were received from Cartosat-2 and Resourcesat-2. But, due to high cloud cover, these datasets could not be interpreted. To avoid cloud problem, microwave data from Indian microwave satellite (RISAT-2) were acquired. Similarly, through an initiative of ICSMD, Radarsat-2 and TerraSAR-X data were provided by Canadian Space Agency and German Aerospace Centre, respectively. However, these microwave datasets could not be interpreted for damage assessment in this area due to: i) unavailability of pre-earthquake microwave data with acquisition parameters similar to the post-earthquake data, and ii) high geometric distortion due to foreshortening and layover effects, which is typical in steep terrains such as the Himalayas.

ISRO and other agencies of ICSMD continued their watch over Sikkim, and first cloud free VHR data for this area were available on 27 September 2011 from WorldView-2. On 30 September 2011, major part of the Sikkim was captured by Cartosat-1. A list of satellite data used for this event is provided in table 1 and the extent of data coverage is shown in figure 1. Apart from high resolution data, medium resolution post-earthquake Landsat-7 ETM+ data covering entire Sikkim area were also analysed for regional assessment. These datasets, although having few patches of cloud, were used for analysis since fast dissemination of results is a priority in any disaster situation. Several pre-earthquake images from same satellites were also used during analysis (Table 1).

Table 1 Satellite data used in the Sikkim earthquake study.

<table>
<tr><th>Satellite</th><th>Date of Acquisition</th><th>Sensor type (resolution)</th><th>Data type</th><th>No. of Scenes</th><th>Source</th></tr>
<tr><td rowspan="3">Cartosat-1</td><td>05 October 2011</td><td rowspan="3">Panchromatic (2.5 m)</td><td rowspan="3">Stereoscopic</td><td>3</td><td rowspan="3">ISRO</td></tr>
<tr><td>30 September 2011</td><td>3</td></tr>
<tr><td>22 March 2011</td><td>3</td></tr>
</table>

GeoEye-1	05 October 2011	Panchromatic (38 cm) Multispectral (1.5 m)	Monoscopic	62	USGS
QuickBird-2	29 September 2011	Panchromatic (90 cm) Multispectral (2.8 m)	Monoscopic	18	USGS
WorldView-2	27 September 2011	Panchromatic (60 cm) Multispectral (2.4 m)	Monoscopic	8	USGS
WorldView-1	26 April 2011			22	
Resourcesat-2 LISS-IV Mx	03 October 2011	Multispectral (5.8 m)	Monoscopic	1	ISRO
Resourcesat-2 LISS-III	13 March 2011	Multispectral (23.5 m)	Monoscopic	1	ISRO
Landsat-5 TM	12 September 2011	Multispectral (30 m)	Monoscopic	1	USGS
Landsat-7 ETM+	06 October 2011	Panchromatic (15 m) Multispectral (30 m)	Monoscopic	1	USGS

4. Methodology

4.1. Data processing

Stereoscopic Cartosat-1 data were processed first for a 3D visualisation of the earthquake affected area. Cartosat-1 has two panchromatic (PAN) cameras; PAN aft (-5°) and PAN fore

(+26°), and are provided with rational polynomial coefficients (RPCs), which can be used for photogrammetric processing and subsequent generation of digital elevation models (DEMs) and orthorectified images. High planimetric accuracy is desirable for products derived from satellite data for disaster support purposes (Voigt et al., 2007). In order to improve the planimetric accuracy of Cartosat-1 data, we used existing ground control points collected from a differential GPS (DGPS) survey (Baltsavias et al., 2008; Martha et al., 2010). The stereo pairs were processed and block triangulation was performed using Leica Photogrammetric Suite (LPS) software. Subsequently, a 10 m DEM and Cartosat-1 orthorectified images were generated.

Pan-sharpening and contrast enhancement were the other data processing techniques attempted in this study. For example, pan-sharpening of the GeoEye-1 panchromatic image (38 cm) with its multispectral image (1.5 m) resulted in a 38 cm (resolution) post-disaster colour image that provided information about the damages those were intuitive and detailed.

4.2. Data analysis

A combination of panchromatic, multispectral, monoscopic and stereoscopic data were used for image interpretation. Visual change analysis by comparing post-earthquake images with the pre-earthquake images was mainly used to find earthquake induced changes in the terrain. 3D visual interpretation of Cartosat-1 images was carried out using the feature extraction tool of ERDAS software. While Cartosat-1 was helpful for damage assessment due to the 3D visualisation of the terrain; GeoEye-1, WorldView-2 and QuickBird-2 data were able to provide details of the changes on the ground after the earthquake. The focus of the image interpretation was to find out the damage to infrastructures (roads, bridges and dam sites), buildings, terrain in the form of landslides and any other economic losses.

5. Results and discussion

5.1. Post-earthquake landslide inventory

The Sikkim Himalayas is susceptible landslide occurrences (Mehrotra et al., 1996). Landslides cause exposure of fresh rocks and soils, and removal of vegetations. These effects can be seen clearly in the post-earthquake image in the form of high image brightness. Some other features such as barren land, roads and river sands also provide similar tone and can incorrectly be interpreted as landslides. Due to several developmental activities in this area, road cuttings can be falsely interpreted as post-earthquake landslides since they also give high brightness as landslides (Fig. 2). However, a careful analysis of the image tone in association with texture, shape and pattern can help accurate identification of landslides.

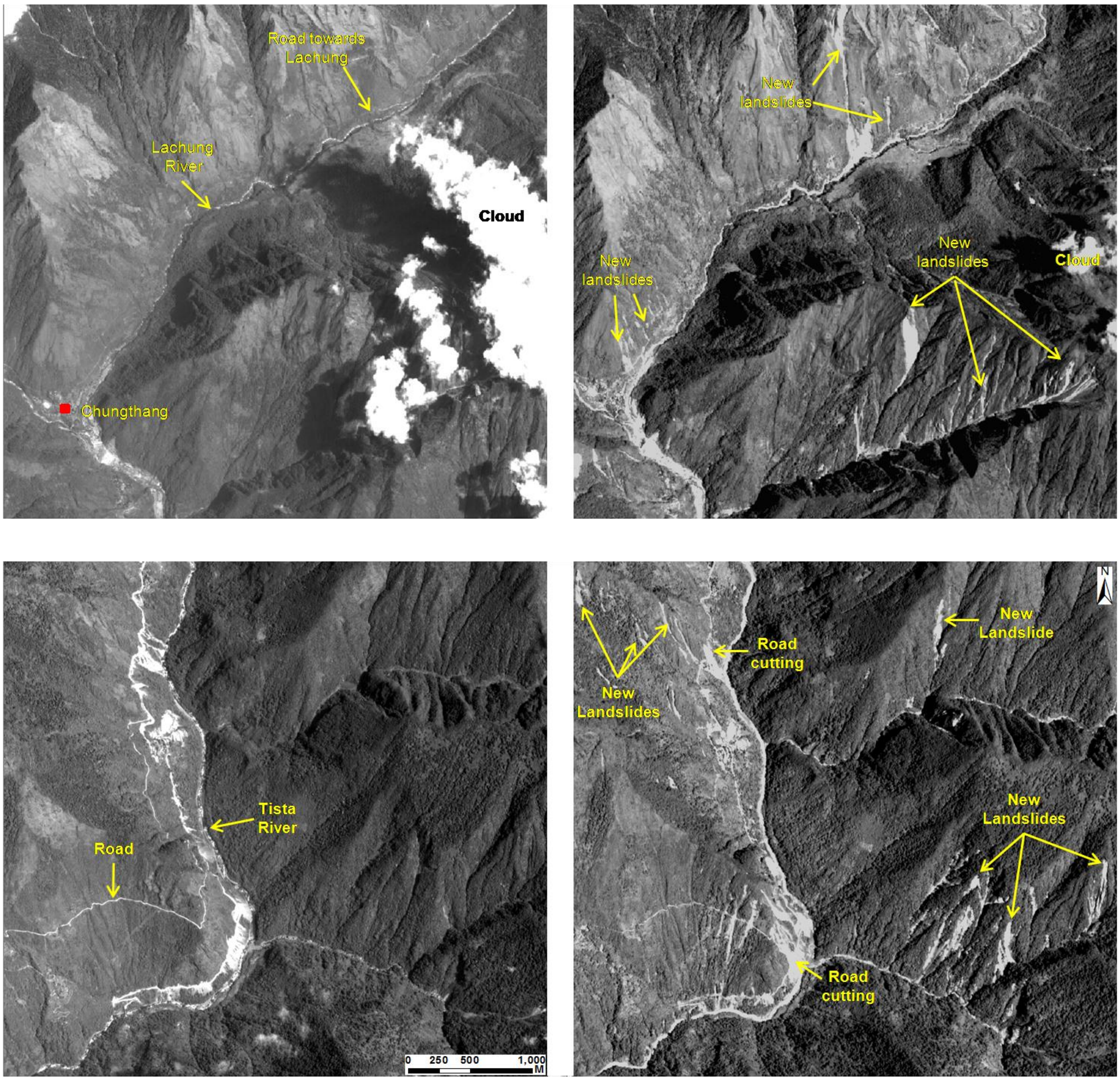

Fig. 2. New landslides mapped from Cartosat-1 image in an area east of Mangan (bottom) and near Chungthang (top). Pre- and post-earthquake images are shown in left and right, respectively. Road cuttings can be seen in both images.

Demarcation of landslides as polygons, through ideal, was avoided in this study since it was time consuming (Voigt et al., 2007). Therefore, landslide locations were marked as points. The points were placed in the zones of initiation of the landslides by using similar method applied by Gorum et al. (2011) for the 2008 Wenchuan earthquake. Most of the landslides were of shallow transalational nature, which can be interpreted from its size and elongated shape. However, large rock falls and rock slides were also observed in this area. Occurrence of rock falls and rock slides are typical after an earthquake (Jibson et al., 2006). Old landslides, reactivated due to the earthquake, were identified and mapped as new landslides (Fig. 3). Total 1196 new landslides were mapped using post-earthquake satellite images (Fig. 4). The geographic location of all landslides is given in Annexure-I.

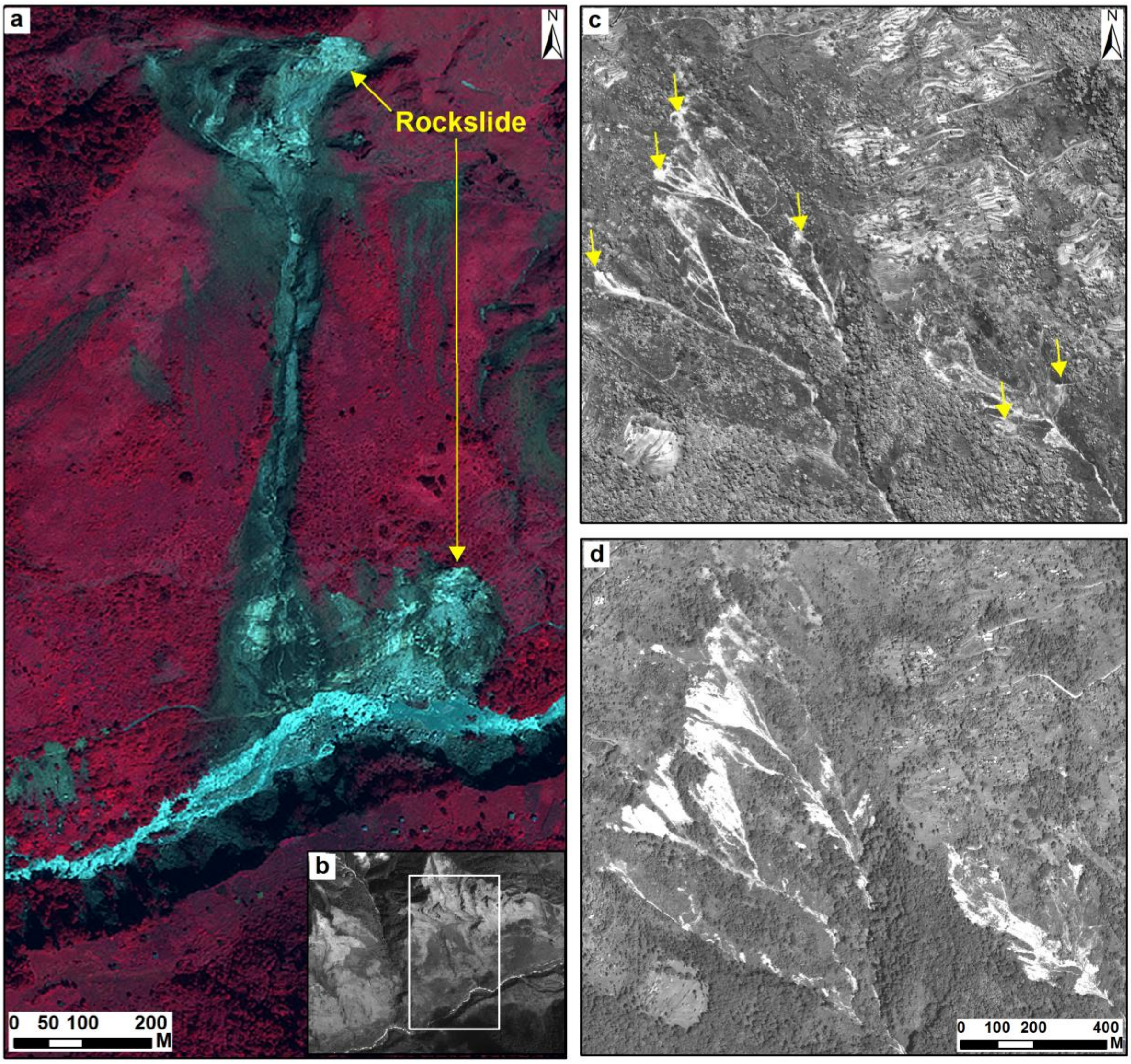

Fig. 3. Different types of landslides. a. Post-earthquake WorldView-2 false colour composite of a large rock slide, b. Pre-earthquake Cartosat-1 image. Rectangle inside shows the location of WorldView-2 image, c. Old landslides (shown with yellow arrows) as seen in the pre-earthquake WorldView-1 image, and d. Reactivation of old landslides seen from post-earthquake GeoEye-1 image.

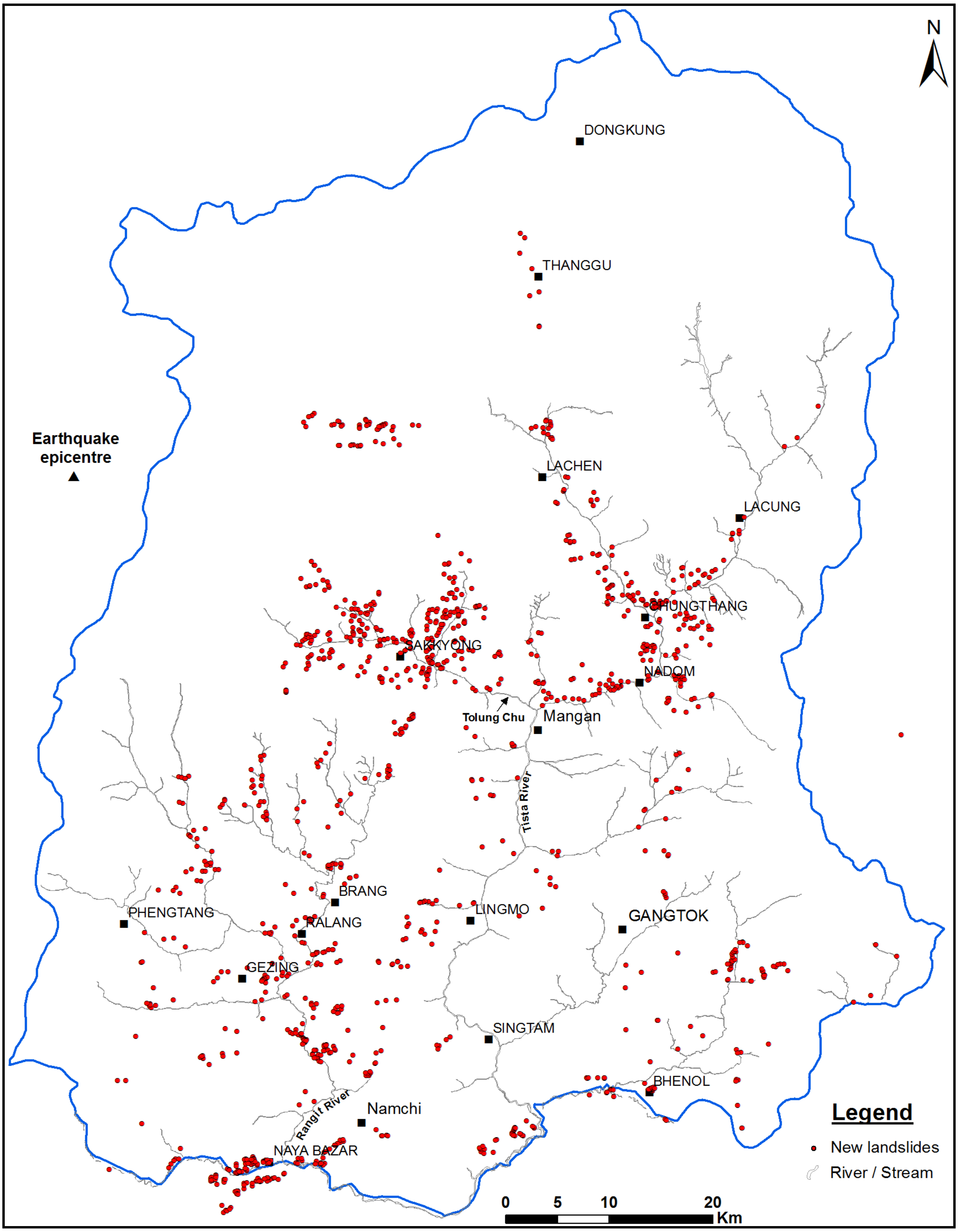

Fig. 4. Post-earthquake landslide inventory created from VHR images. Landslide locations are marked as dots.

5.2. Infrastructural damage

Several parts of Sikkim remained inaccessible for many days after the earthquake mainly due to the blockage of roads. It was possible to identify such areas using VHR images. Figure 5 shows how a part of the road previously affected by landslides was again affected by new landslides after the earthquake. Areas such as Mangan and Chungthang, which are close to the earthquake epicentre were severely affected and several roads were either destroyed or blocked by the debris (Figure 6).

Another important infrastructure, which is of concern, is the presence of two hydro electric dams. One across Tista river and the other across Rangit river (tributary to Tista). No major damage was observed from the VHR images in the dam area except the occurrence landslides in the reservoir catchment area (Fig. 7). These landslides will contribute sediments to the reservoir after rainfall resulting in enhancement of siltation related problems. Apart from blocking roads, landslides are capable of blocking rivers (Dunning et al., 2007). In this analysis no such major blockages and creation of temporary reservoirs were observed except few minor ones in the upstream of Tolung Chu, which is a tributary to the Tista river.

5.3. Building damage

As per the news report, some buildings collapsed and several developed cracks due to the earthquake. During the analysis of VHR images of some of the major settlements in this area, we could not find any noticeable change. However, one village was completely destroyed by a large landslide in the Tolung chu (river) upstream areas (Fig. 8). A report suggests 120 people are missing from this village. Similarly, in the Chungthang area, buildings in the run out zones of landslides, were also observed.

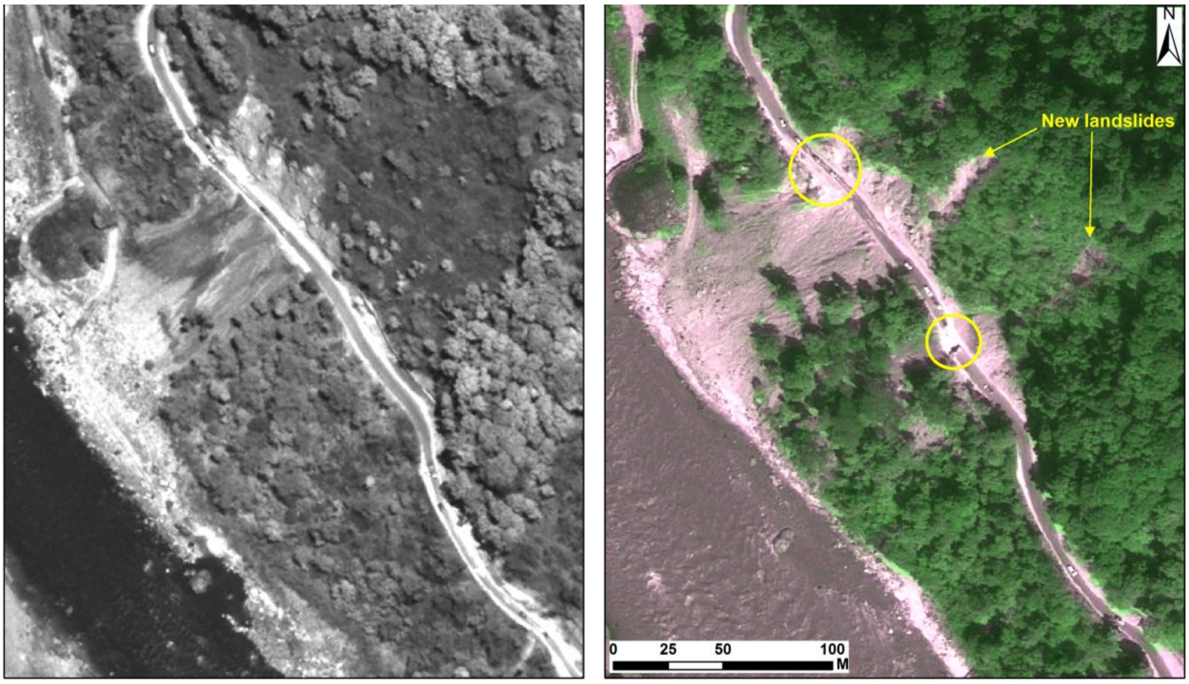

Fig. 5. Blockage of the road near the Tista river due to landslides. The debris was cleared after the earthquake to allow movement of vehicles since it is a major road in this area. Left - pre-earthquake WorldView-2 image, and right - post-earthquake pansharpened GeoEye-1 image shown with natural colour composite.

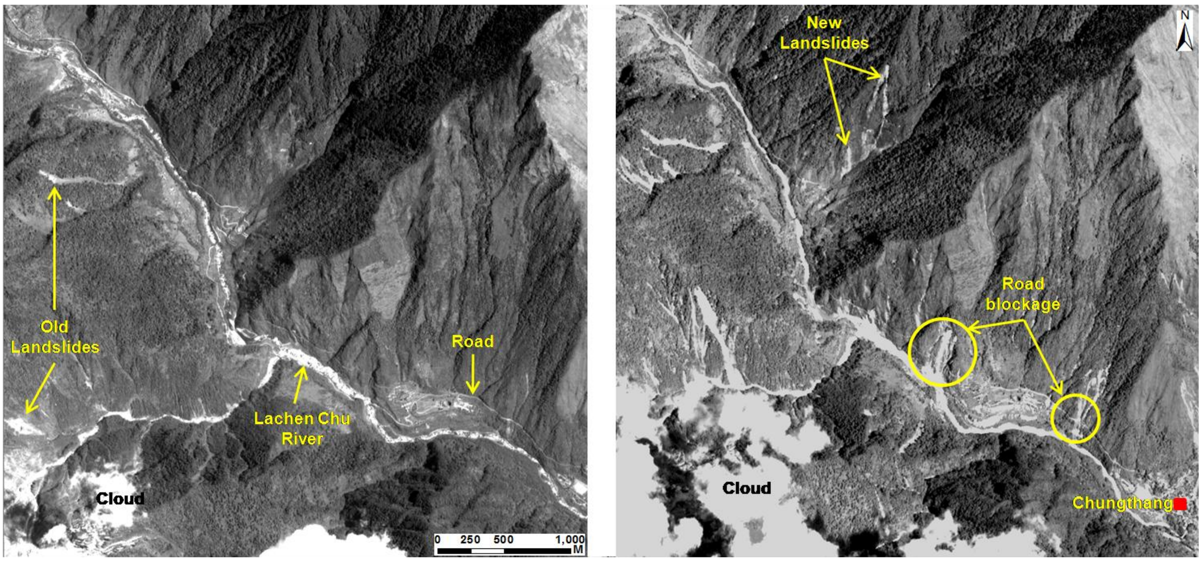

Fig. 6. Parts of road completely destroyed by landslides triggered due to the earthquake near Chungthang area in north Sikkim. Pre- and post-earthquake Cartosat-1 images are shown in left and right, respectively.

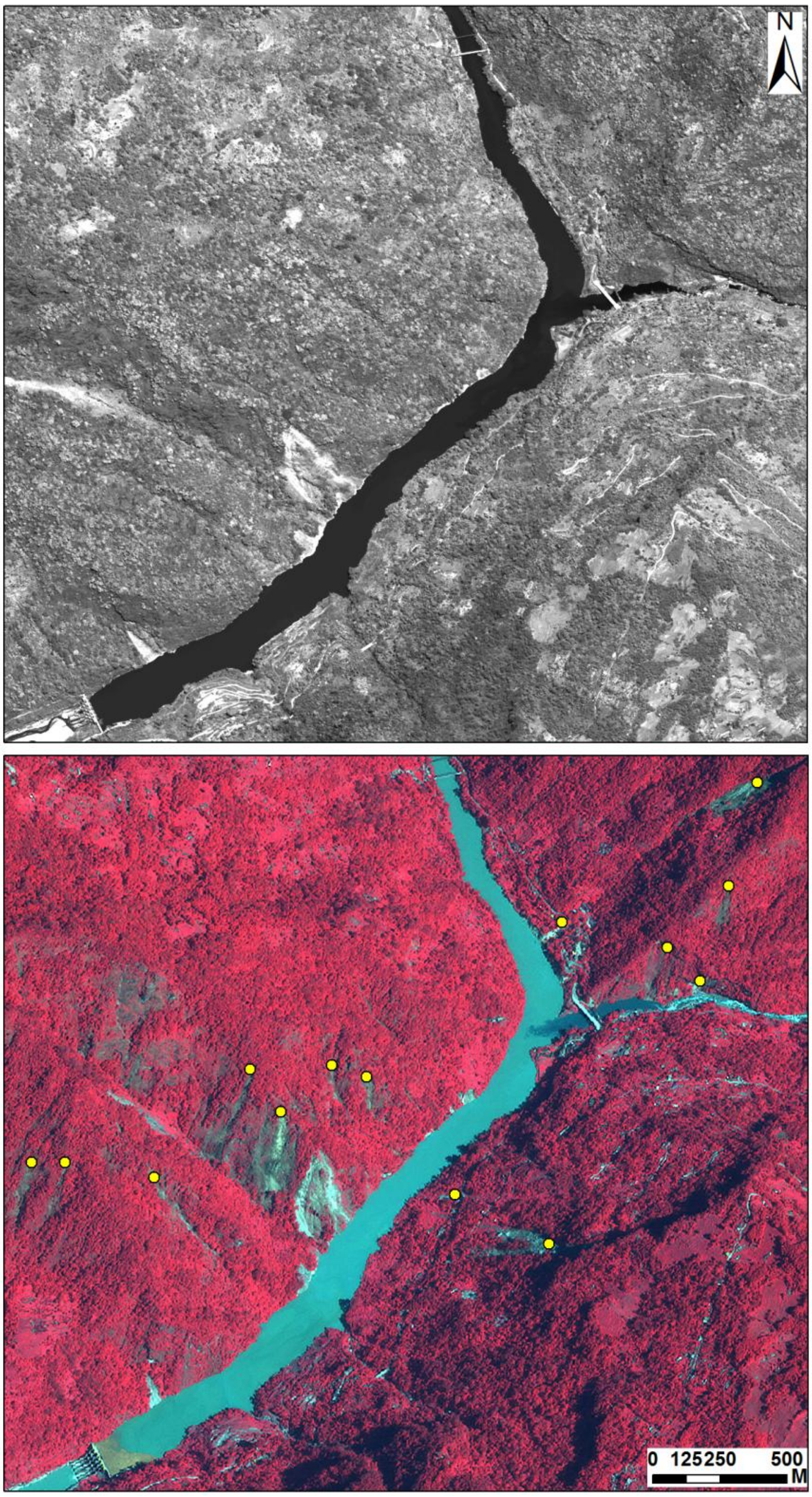

Fig. 7. False colour composite of post-earthquake QuickBird-2 multispectral image in the bottom showing landslides in the reservoir area of a dam across Tista river. Pre-earthquake panchromatic WorldView-1 is shown in the top. High reflectance of water in the reservoir in the post-earthquake image is due to its sediment richness. New landslides triggered after the earthquake are shown with yellow dots.

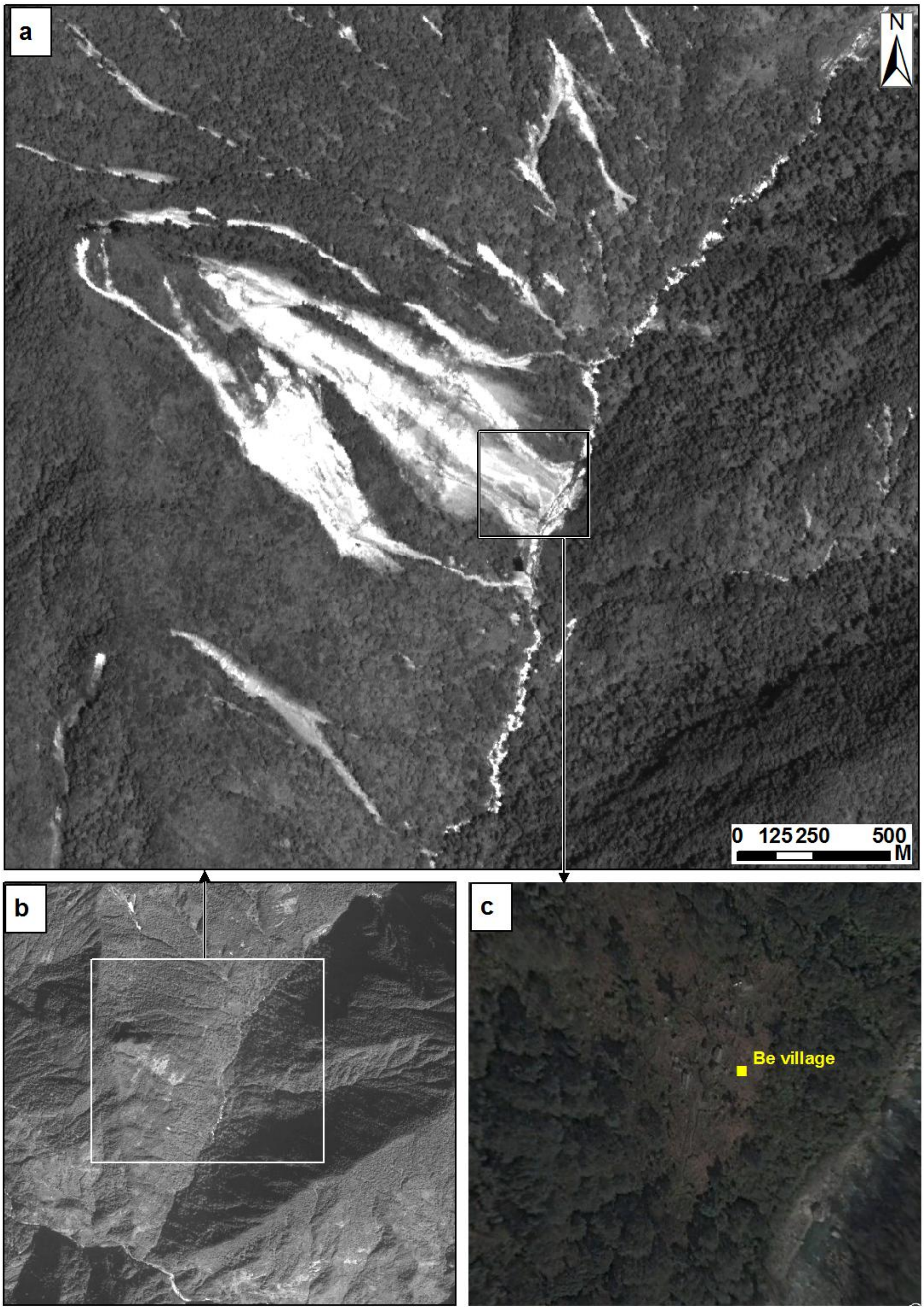

Fig. 8. Be village landslide in north Sikkim. a. Post-earthquake Cartosat-1 image, b. Pre-earthquake Cartosat-1 image, and c. Google Earth image of 2010 in which individual building can be seen.

5.4. Agricultural damage

Agricultural lands in steep Himalayan terrain are limited and precious. Some of these lands in southern Sikkim are well known for tea cultivation. Periphery of the tea gardens, which is mostly in the steep slopes were affected by landslides (Fig. 9).

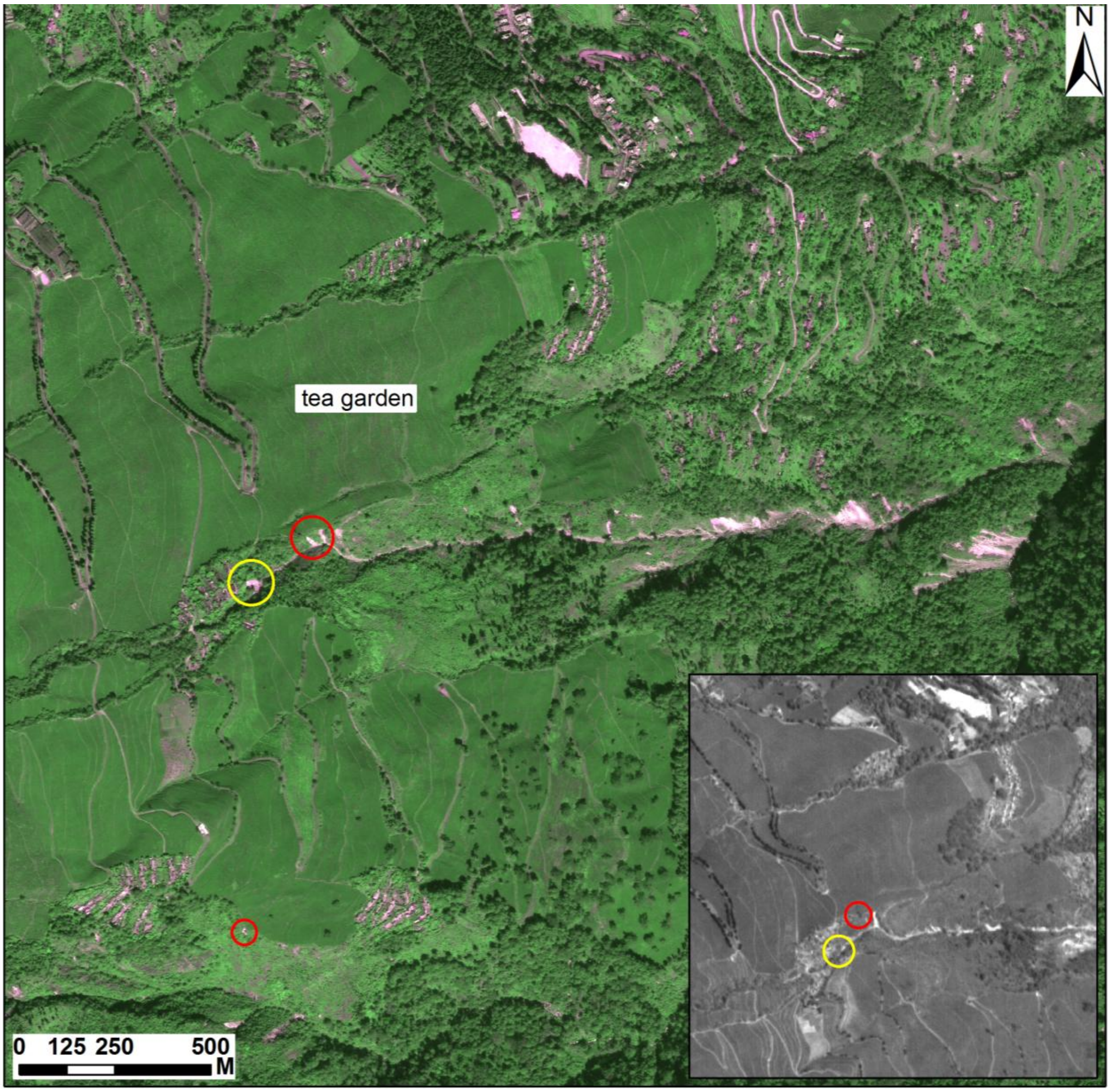

Fig. 9. Post-earthquake natural colour composite of pansharpened GeoEye-1 image showing a tea garden in south Sikkim. Inset shows pre-earthquake Cartosat-1 image. Peripheral part of the tea garden including the small settlement where tea workers mainly stay were affected by landslides (shown with yellow circle) triggered due to the earthquake. New landslides are highlighted with red circles.

5.5. Geological assessment

High magnitude earthquakes could cause reactivation of faults (Vinod Kumar et al., 2006). Stereoscopic interpretation of satellite images were used previously to demarcate fault scarps (Salvi, 1995). Fua et al. (2004) have shown the usefulness of ASTER 3D images for mapping active faults due to the 2003 Bam earthquake in Iran. Similarly, Vinod Kumar et al. (2006) have shown reactivation of Jhelum fault due to the 2005 Kashmir earthquake. Linear disposition of landslide along a prominent lineament is one of the key criteria to identify locations of fault reactivation after the earthquake. In this area, one of the N-S oriented scarp, alignment of large post-earthquake rock slides was prominently observed during the stereoscopic interpretation of Cartosat-1, which suggests reactivation of the fault (Fig. 10).

Similarly, areas west of Nayabazar in the border between West Bengal and Sikkim states witnessed occurrence of 113 new landslides after the earthquake (Fig. 11). These landslides occurred along the Rangbang and Chhota Rangit river valleys, which represents MCT on the surface. Linear disposition of these landslides along an existing fault suggests its reactivation due to the earthquake. Further in Lachen, Chungthang and Nadom areas, several landslides are triggered after the earthquake in the river valley which coincides with the fault mapped by GSI (2000) (Fig. 4).

Areas close to the earthquake epicentre generally witness occurrence of many landslides. To verify this, we compared the post-earthquake landslide inventory map with the shake map published by USGS (2011). Figure 4 shows clusters of landslides in areas close to the earthquake epicentre west of Mangan in the Tolung Chu (river) valley in comparison to areas away from the epicentre such as Gangtok and Singtam. The gap in landslide occurrences in the east of the epicentre corresponds to Kanchejunga peak areas, which are permanently snow covered. During the analysis of post-earthquake Landsat-7 ETM+ data on the Nepal side, we also observed occurrence of landslides in areas close to the epicentre. These observations suggest a good match between the landslide inventory and shake map.

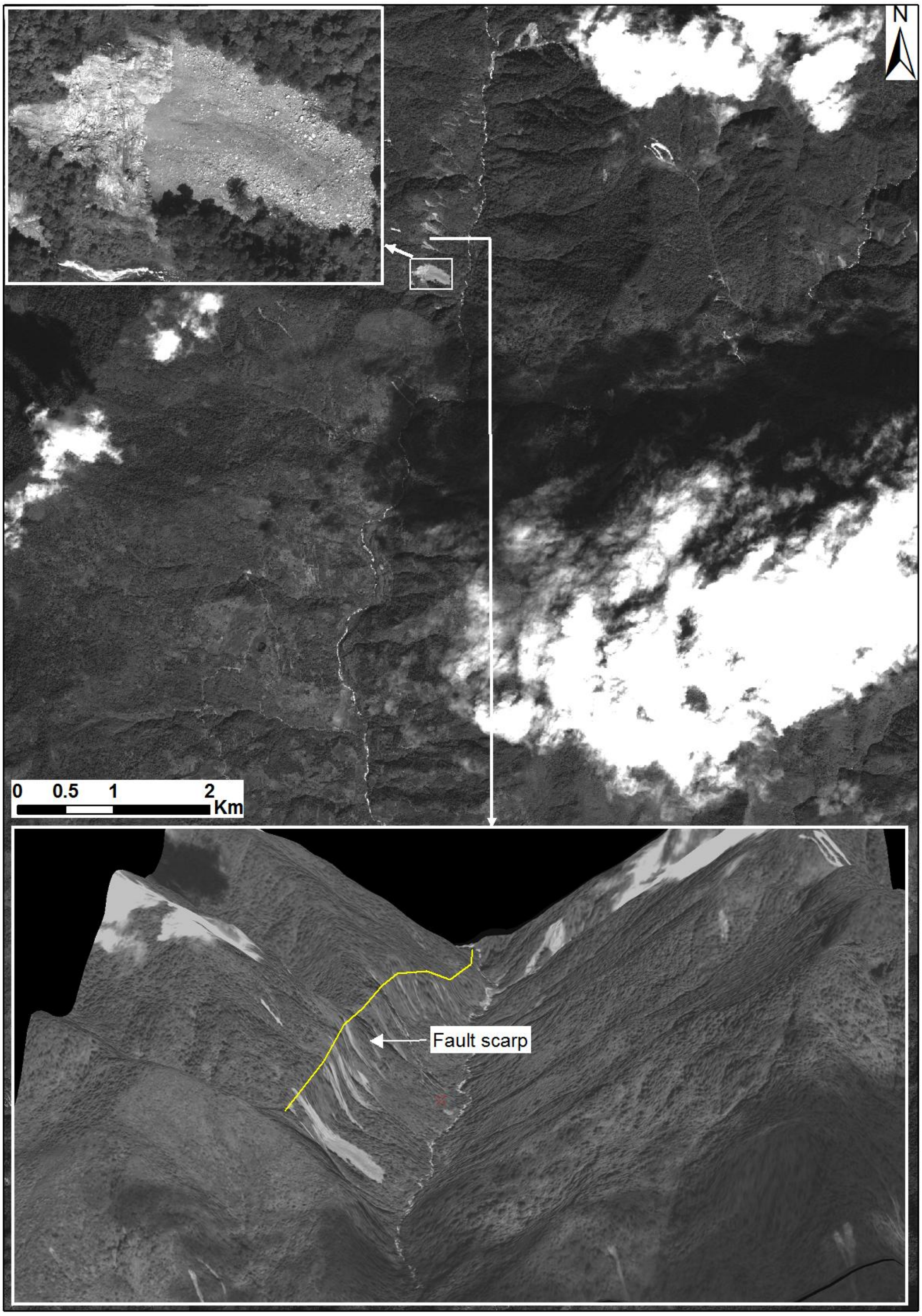

Fig. 10. Post-earthquake panchromatic image of GeoEye-1. Inset (upper) shows a large rock fall. Source area of the rock fall as well as the debris could be seen clearly in the VHR image. Inset (lower) shows 3D perspective of the fault scarp with the yellow line marked on a prominent break-in-slope. Linear disposition of large rock falls along the scarp suggests reactivation of the fault.

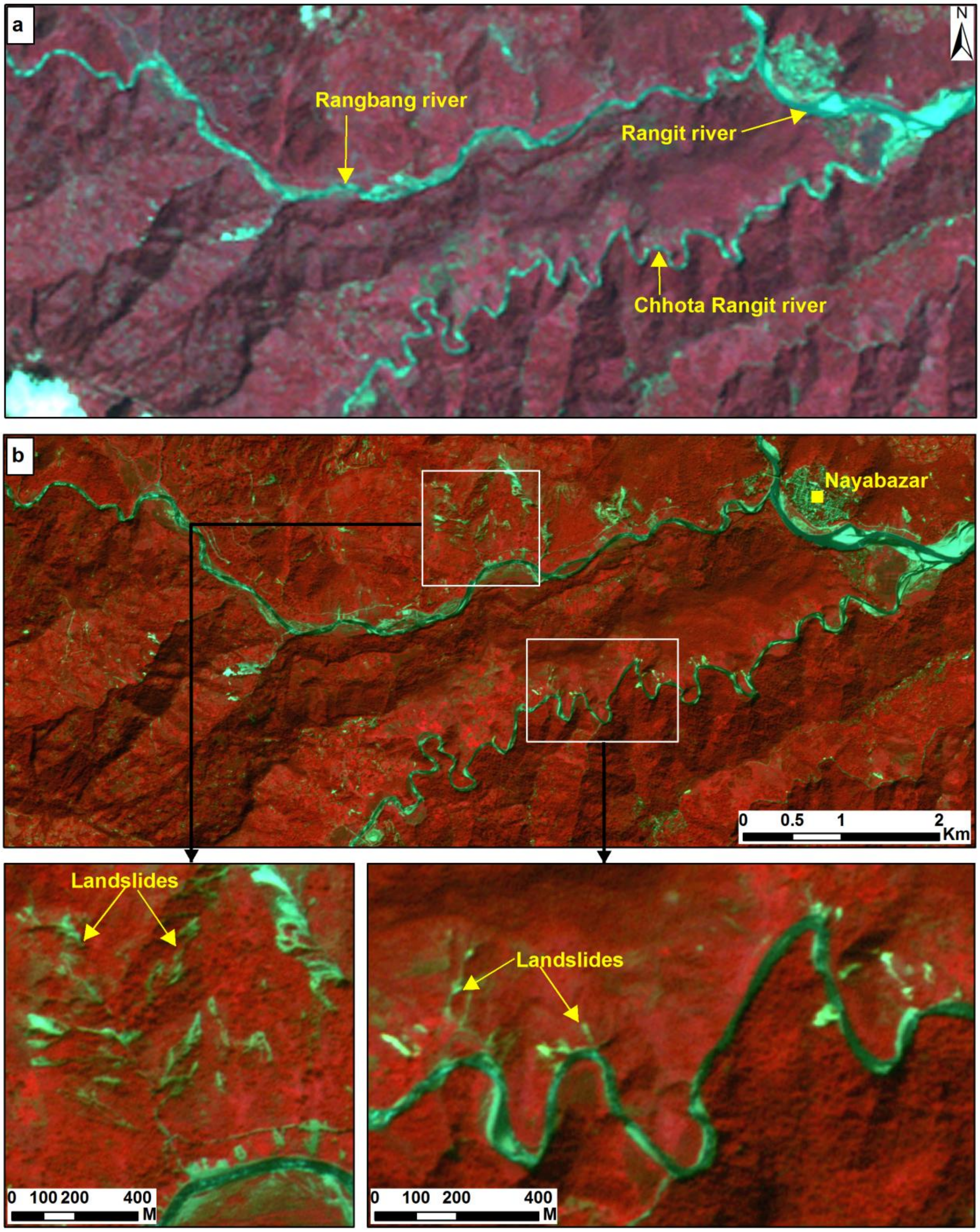

Fig. 11. Landslides triggered along MCT in the Nayabazar area. a. Landsat-5 TM image acquired six days before the earthquake shows minor presence of landslides, b. Resourcesat-2 LISS IV Mx image showing several landslides triggered due to the earthquake along Rangbang and Chhota Rangit rivers.

6. Conclusions

This report highlights the importance of VHR images in a disaster situation. The main contribution of the report is rapid assessment of an area (4105 km^2) in Sikkim using 123 scenes of images from eight satellites. Acquisition of satellite images under the coordinated effort under ICSMD was very helpful since the data for the affected area was made available in short time, which helped in rapid assessment and quick dissemination of results. Preliminary results highlighting the affected areas were hosted on 04 October 2011 in the NRSC website (www.nrsc.gov.in) for information to general public.

A total of 1196 new landslides (including reactivated landslides) were mapped in the Sikkim area. Mangan and Chungthang areas in north Sikkim were found to be severely affected by landslides. Be village, west of Mangan was completely destroyed by a large rock slide. Many roads along Tista river and its tributaries, were either blocked or completely dislodged by landslides. Landslides were also mapped in the reservoir catchment areas which may cause siltation related problems in future.

3D visualisation coupled with detail information of the terrain provided by VHR images were helpful to identify locations of rock fall along an escarpment suggesting activation of faults due to the earthquake. Linear disposition of landslides along existing faults showed their reactivation due to the earthquake. The landslide inventory map prepared from VHR images matched well with the earthquake shake map of USGS.

Although results from the rapid assessment of Sikkim earthquake were presented in this report, availability of cloud free data nine days after the earthquake caused the delay in carrying out the damage assessment. Microwave data, although, available immediately after the earthquake could not be interpreted due to foreshortening and layover effects, which are inherent problems in rugged terrains. Nevertheless, the report presented a rapid and detail assessment of vastly inaccessible areas in Sikkim which otherwise would have been difficult.

7. References

Arciniegas, G.A., Bijker, W., Kerle, N., & Tolpekin, V.A. (2007). Coherence- and Amplitude-Based Analysis of Seismogenic Damage in Bam, Iran, Using ENVISAT ASAR Data. *IEEE Transactions on Geoscience and Remote Sensing*, *45*, 1571-1581

Baltsavias, E., Kocaman, S., & Wolff, K. (2008). Analysis of Cartosat-1 images regarding image quality, 3D point measurement and DSM generation. *The Photogrammetric Record*, *23*, 305-322

Di, B., Zeng, H., Zhang, M., Ustin, S.L., Tang, Y., Wang, Z., Chen, N., & Zhang, B. (2010). Quantifying the spatial distribution of soil mass wasting processes after the 2008 earthquake in Wenchuan, China A case study of the Longmenshan area. *Remote Sensing of Environment, 114*, 761-771

Dunning, S.A., Mitchell, W.A., Rosser, N.J., & Petley, D.N. (2007). The Hattian Bala rock avalanche and associated landslides triggered by the Kashmir Earthquake of 8 October 2005. *Engineering Geology, 93*, 130-144

Fua, B., Ninomiyab, Y., Leib, X., Todaa, S., & Awata, Y. (2004). Mapping active fault associated with the 2003 Mw 6.6 Bam (SE Iran) earthquake with ASTER 3D images. *Remote Sensing of Environment, 94*, 153-157

Gamba, P., Dell'Acqua, F., & Trianni, G. (2007). Rapid Damage Detection in the Bam Area Using Multitemporal SAR and Exploiting Ancillary Data. *IEEE Transactions on Geoscience and Remote Sensing, 45*, 1582-1589

Ghosh, S., Gunther, A., Carranza, E.J.M., van Westen, C.J., & Jetten, V.G. (2010). Rock slope instability assessment using spatially distributed structural orientation data in Darjeeling Himalaya (India). *Earth Surf. Process. Landforms*, *35*, 1773-1792

Gorum, T., Fan, X., van Westen, C.J., Huang, R.Q., Xu, Q., Tang, C., & Wang, G. (2011). Distribution Pattern of Earthquake-induced Landslides Triggered by the 12 May 2008 Wenchuan Earthquake. *Geomorphology*, *133*, 152-167

GSI (2000). *Seismotectonic atlas of India and its environs*. Calcutta, India: Geological Survey of India

Jibson, R.W., Harp, E.L., Schulz, W., & Keefer, D.K. (2006). Large rock avalanches triggered by the M 7.9 Denali Fault, Alaska, earthquake of 3 November 2002. *Engineering Geology, 83*, 144-160

Kayal, J.R. (2001). Microearthquake activity in some parts of the Himalayas and the tectonic model. *Tectonophysics, 339*, 331-351

Martha, T.R., Kerle, N., van Westen, C.J., Jetten, V., & Vinod Kumar, K. (2010). Effect of sun elevation angle on DSMs derived from Cartosat-1 data. *Photogrammetric Engineering and Remote Sensing, 76*, 429-438

Mehrotra, G.S., Sarkar, S., Kanungo, D.P., & Mahadevaiah, K. (1996). Terrain analysis and spatial assessment of landslide hazards in parts of Sikkim Himalaya. *Journal of the Geological Society of India, 47*, 491-498

Metternicht, G., Hurni, L., & Gogu, R. (2005). Remote sensing of landslides: An analysis of the potential contribution to geo-spatial systems for hazard assessment in mountainous environments. *Remote Sensing of Environment, 98*, 284-303

Raju, P.S., Rao, N.P., Singh, A., & Ravi Kumar, A. (2007). The 14 February 2006 Sikkim earthquake of magnitude 5.3. *Current Science, 93*, 848-850

Ray, P.K.C., Parvaiz, I., Jayangondaperumal, R., Thakur, V.C., Dadhwal, V.K., & Bhat, F.A. (2009). Analysis of seismicity-induced landslides due to the 8 October 2005 earthquake in Kashmir Himalaya. *Current Science, 97*, 1742-1755

Salvi, S. (1995). Analysis and interpretation of Landsat synthetic stereo pair for the detection of active fault zones in the Abruzzi region (Central Italy). *Remote Sensing of Environment, 53*, 165-163

Stumpf, A., & Kerle, N. (2011). Object-oriented mapping of landslides using random forests. *Remote Sensing of Environment, DOI:10.1016/j.rse.2011.05.013*

Tralli, D.M., Blom, R.G., Zlotnicki, V., Donnellan, A., & Evans, D.L. (2005). Satellite remote sensing of earthquake, volcano, flood, landslide and coastal inundation hazards. *ISPRS Journal of Photogrammetry and Remote Sensing, 59*, 185-198

USGS (2011). Shake map: India-Nepal border region. Available online at: http://earthquake.usgs.gov/earthquakes/shakemap/global/shape/c0005wg6/#Instrumental_Intensity.

Vinod Kumar, K., Martha, T.R., & Roy, P.S. (2006). Mapping damage in the Jammu and Kashmir caused by 8 October 2005 Mw 7.3 earthquake from the Cartosat–1 and Resourcesat–1 imagery. *International Journal of Remote Sensing, 27*, 4449-4459

Voigt, S., Kemper, T., Riedlinger, T., Kiefl, R., Scholte, K., & Mehl, H. (2007). Satellite Image Analysis for Disaster and Crisis-Management Support. *IEEE Transactions on Geoscience and Remote Sensing, 45*, 1520-1528

Wang, F., Cheng, Q., Highland, L., Miyajima, M., Wang, H., & Yan, C. (2009). Preliminary investigation of some large landslides triggered by the 2008 Wenchuan earthquake, Sichuan Province, China. *Landslides, 6*, 47-54

Annexure - I

Location of Landslides

Sl. No	X_Long	Y_Lat
1	88.5253	27.1573
2	88.5246	27.1583
3	88.5234	27.1589
4	88.5177	27.1637
5	88.4442	27.2379
6	88.4405	27.2356
7	88.4334	27.2300
8	88.4312	27.2305
9	88.4321	27.2270
10	88.3923	27.2707
11	88.7379	27.6875
12	88.6509	27.6220
13	88.6469	27.6160
14	88.6479	27.6158
15	88.6485	27.6156
16	88.6487	27.6137
17	88.6532	27.6102
18	88.6518	27.6110
19	88.6541	27.6126
20	88.6540	27.6133
21	88.6546	27.6151
22	88.6546	27.6132
23	88.6565	27.6138
24	88.6556	27.6135
25	88.6497	27.6113
26	88.6478	27.6096
27	88.6481	27.6099
28	88.6482	27.6100
29	88.6503	27.6100
30	88.6531	27.5975
31	88.6541	27.5992
32	88.6686	27.6140
33	88.6679	27.6229
34	88.6604	27.6155
35	88.6612	27.6154
36	88.6850	27.6387
37	88.6920	27.6311
38	88.6887	27.6293
39	88.6833	27.6267
40	88.7060	27.6409
41	88.7032	27.6353
42	88.6972	27.6376
43	88.6921	27.6418
44	88.6988	27.6382
45	88.6766	27.6374
46	88.6764	27.6441
47	88.6770	27.6444
48	88.6676	27.6337
49	88.6413	27.6119
50	88.6381	27.6160
51	88.6371	27.6170
52	88.6361	27.6170
53	88.6292	27.6161
54	88.6276	27.6178
55	88.6329	27.6230
56	88.6268	27.6319
57	88.6241	27.6292
58	88.6223	27.6398
59	88.6083	27.6183
60	88.6074	27.6180
61	88.6040	27.6207
62	88.6037	27.6192
63	88.6030	27.6135
64	88.6029	27.6147
65	88.6085	27.6297
66	88.6071	27.6300
67	88.6063	27.6289
68	88.6050	27.6278
69	88.6033	27.6271
70	88.6230	27.6075
71	88.6191	27.6028
72	88.6007	27.6345
73	88.5944	27.6409
74	88.5891	27.6574
75	88.5959	27.6571
76	88.5939	27.6558
77	88.6010	27.6449
78	88.6019	27.6452
79	88.5775	27.6538
80	88.5715	27.6528

Sl. No	X_Long	Y_Lat
81	88.5709	27.6681
82	88.5674	27.6673
83	88.5673	27.6681
84	88.5681	27.6525
85	88.5667	27.6739
86	88.5654	27.6738
87	88.5635	27.6693
88	88.5913	27.7111
89	88.5905	27.6993
90	88.5884	27.7030
91	88.5885	27.7040
92	88.5941	27.7046
93	88.5472	27.7621
94	88.5636	27.7245
95	88.5660	27.7244
96	88.5615	27.7123
97	88.5618	27.7133
98	88.5621	27.7137
99	88.5555	27.7019
100	88.5535	27.7025
101	88.6404	27.5934
102	88.6425	27.5934
103	88.6450	27.5951
104	88.6513	27.5885
105	88.6441	27.5758
106	88.6450	27.5759
107	88.6382	27.5778
108	88.6394	27.5722
109	88.6409	27.5727
110	88.6371	27.5639
111	88.6449	27.5641
112	88.6472	27.5715
113	88.6468	27.5770
114	88.6482	27.5765
115	88.6487	27.5749
116	88.6372	27.5754
117	88.6405	27.5771
118	88.6413	27.5776
119	88.6348	27.5699
120	88.6849	27.6000
121	88.6777	27.5941
122	88.6841	27.5913
123	88.7043	27.5900
124	88.7018	27.5902

Sl. No	X_Long	Y_Lat
125	88.7020	27.5931
126	88.6956	27.5965
127	88.6911	27.5931
128	88.7028	27.5767
129	88.6949	27.5825
130	88.6879	27.6010
131	88.6873	27.5909
132	88.6729	27.5906
133	88.6797	27.5993
134	88.6788	27.5992
135	88.6808	27.6024
136	88.7091	27.6419
137	88.7059	27.6172
138	88.7074	27.6151
139	88.7174	27.6501
140	88.7252	27.6682
141	88.7326	27.6731
142	88.7329	27.6761
143	88.7264	27.6733
144	88.7263	27.6738
145	88.4686	27.6527
146	88.4749	27.6129
147	88.4766	27.6130
148	88.4968	27.5728
149	88.5279	27.5705
150	88.5254	27.5813
151	88.5278	27.5823
152	88.5353	27.5894
153	88.5382	27.5885
154	88.6705	27.5727
155	88.6711	27.5712
156	88.6793	27.5758
157	88.6696	27.5653
158	88.6678	27.5685
159	88.6079	27.6558
160	88.6085	27.6629
161	88.4959	27.5447
162	88.6668	27.5199
163	88.6843	27.5292
164	88.6621	27.5305
165	88.4879	27.4478
166	88.5508	27.3943
167	88.5522	27.3984
168	88.5461	27.3984

Sl. No	X_Long	Y_Lat
169	88.5087	27.3967
170	88.4548	27.3523
171	88.4301	27.5782
172	88.4263	27.5687
173	88.4288	27.5674
174	88.4301	27.5691
175	88.4311	27.5706
176	88.4707	27.5741
177	88.4617	27.5580
178	88.4532	27.5472
179	88.4280	27.5589
180	88.4238	27.5434
181	88.4731	27.5393
182	88.4703	27.5415
183	88.4844	27.5417
184	88.4870	27.5403
185	88.4981	27.5493
186	88.4976	27.5700
187	88.4956	27.5712
188	88.5322	27.5459
189	88.5342	27.5467
190	88.5347	27.5450
191	88.5396	27.5460
192	88.5392	27.5447
193	88.5334	27.5690
194	88.5422	27.5314
195	88.5471	27.5328
196	88.5383	27.5257
197	88.5442	27.5360
198	88.5529	27.5299
199	88.5682	27.5313
200	88.5875	27.5340
201	88.5903	27.5349
202	88.5939	27.5363
203	88.6033	27.5402
204	88.6151	27.5418
205	88.6138	27.5411
206	88.6130	27.5407
207	88.6125	27.5402
208	88.6110	27.5412
209	88.6114	27.5418
210	88.6068	27.5438
211	88.6054	27.5385
212	88.6063	27.5525

Sl. No	X_Long	Y_Lat
213	88.6152	27.5459
214	88.6220	27.5452
215	88.6091	27.5393
216	88.6082	27.5384
217	88.6007	27.5429
218	88.6038	27.5470
219	88.5942	27.5390
220	88.5945	27.5437
221	88.5779	27.5611
222	88.5685	27.5491
223	88.5669	27.5481
224	88.6418	27.5468
225	88.6430	27.5475
226	88.6418	27.5505
227	88.6520	27.5530
228	88.6512	27.5540
229	88.6735	27.5473
230	88.6728	27.5467
231	88.6762	27.5489
232	88.6772	27.5466
233	88.6732	27.5493
234	88.6718	27.5501
235	88.6704	27.5494
236	88.6684	27.5492
237	88.6671	27.5505
238	88.6687	27.5468
239	88.6732	27.5411
240	88.6735	27.5439
241	88.6868	27.5303
242	88.7031	27.5323
243	88.7040	27.5331
244	88.6906	27.5228
245	88.6788	27.5183
246	88.6611	27.5305
247	88.6600	27.5267
248	88.6611	27.5280
249	88.5788	27.5298
250	88.5740	27.5311
251	88.5087	27.4906
252	88.5100	27.4909
253	88.5092	27.4909
254	88.5081	27.4929
255	88.4722	27.4995
256	88.4634	27.5072

Sl. No	X_Long	Y_Lat
257	88.5128	27.4626
258	88.4893	27.4475
259	88.4863	27.4482
260	88.5303	27.3819
261	88.5434	27.3753
262	88.5490	27.3674
263	88.5435	27.3698
264	88.6487	27.4595
265	88.6636	27.4486
266	88.6708	27.4513
267	88.6684	27.4517
268	88.6717	27.4827
269	88.6684	27.4815
270	88.6801	27.4682
271	88.6574	27.4256
272	88.6307	27.4188
273	88.6376	27.4339
274	88.6362	27.4331
275	88.6366	27.3981
276	88.6565	27.3569
277	88.6557	27.3591
278	88.6555	27.3605
279	88.6541	27.3620
280	88.6166	27.2982
281	88.5358	27.3489
282	88.5133	27.3422
283	88.4977	27.4080
284	88.4778	27.4029
285	88.4687	27.3543
286	88.4683	27.3542
287	88.4249	27.3559
288	88.4322	27.3566
289	88.4211	27.3558
290	88.4209	27.3564
291	88.4190	27.3556
292	88.4166	27.3555
293	88.4163	27.3550
294	88.4052	27.3368
295	88.4035	27.3345
296	88.4036	27.3425
297	88.6590	27.3934
298	88.6551	27.3974
299	88.6595	27.3940
300	88.4725	27.4454

Sl. No	X_Long	Y_Lat
301	88.4685	27.4619
302	88.4688	27.4610
303	88.4778	27.4618
304	88.4359	27.3831
305	88.3022	27.5803
306	88.3782	27.5793
307	88.2879	27.2942
308	88.3110	27.1829
309	88.3804	27.5834
310	88.3802	27.5844
311	88.3651	27.5887
312	88.3650	27.5897
313	88.3430	27.7544
314	88.3420	27.7546
315	88.3563	27.7547
316	88.3546	27.7548
317	88.3535	27.7543
318	88.3617	27.7537
319	88.3609	27.7538
320	88.3626	27.7537
321	88.3634	27.7545
322	88.3781	27.7577
323	88.3857	27.7553
324	88.3960	27.7598
325	88.4015	27.7545
326	88.4202	27.7709
327	88.4145	27.7713
328	88.3957	27.7703
329	88.3941	27.7672
330	88.3806	27.7687
331	88.3805	27.7683
332	88.3798	27.7681
333	88.3878	27.7726
334	88.3860	27.7723
335	88.3856	27.7713
336	88.3834	27.7714
337	88.3830	27.7707
338	88.3813	27.7706
339	88.3722	27.7744
340	88.3719	27.7727
341	88.3704	27.7726
342	88.3696	27.7715
343	88.3687	27.7768
344	88.3688	27.7761

Sl. No	X_Long	Y_Lat
345	88.3623	27.7723
346	88.3626	27.7701
347	88.3627	27.7693
348	88.3459	27.7722
349	88.3446	27.7712
350	88.3427	27.7750
351	88.3416	27.7757
352	88.3357	27.7723
353	88.3378	27.7726
354	88.3184	27.7825
355	88.3159	27.7806
356	88.3129	27.7799
357	88.3077	27.7753
358	88.3100	27.7713
359	88.3047	27.5843
360	88.3080	27.5861
361	88.3068	27.5858
362	88.3083	27.5883
363	88.3081	27.5900
364	88.3095	27.5903
365	88.3114	27.5890
366	88.3106	27.5871
367	88.2988	27.5812
368	88.3096	27.5701
369	88.3118	27.5712
370	88.3129	27.5720
371	88.3098	27.5652
372	88.3081	27.5597
373	88.3103	27.5630
374	88.3233	27.5754
375	88.3206	27.5688
376	88.3250	27.5682
377	88.3254	27.5690
378	88.3310	27.5699
379	88.3308	27.5733
380	88.3326	27.5763
381	88.3337	27.5751
382	88.3311	27.5913
383	88.3310	27.5852
384	88.3297	27.5900
385	88.3193	27.5925
386	88.3163	27.5892
387	88.3132	27.5869
388	88.3121	27.5825

Sl. No	X_Long	Y_Lat
389	88.3132	27.5849
390	88.3449	27.6074
391	88.3537	27.5918
392	88.3545	27.5904
393	88.3541	27.5893
394	88.3597	27.5935
395	88.3616	27.5924
396	88.3606	27.5922
397	88.3668	27.6139
398	88.3617	27.6084
399	88.3663	27.6080
400	88.3687	27.6082
401	88.3682	27.6067
402	88.3605	27.6017
403	88.3629	27.5980
404	88.3591	27.6113
405	88.3557	27.6165
406	88.3531	27.6120
407	88.3722	27.6112
408	88.3749	27.6153
409	88.3777	27.5937
410	88.3764	27.5953
411	88.3814	27.5928
412	88.3842	27.5851
413	88.3845	27.5843
414	88.3880	27.5857
415	88.3806	27.5798
416	88.4021	27.5848
417	88.4057	27.5832
418	88.3999	27.5728
419	88.4045	27.5749
420	88.4050	27.5752
421	88.4097	27.5915
422	88.4119	27.5899
423	88.4099	27.5893
424	88.4101	27.5893
425	88.4108	27.5878
426	88.4112	27.5928
427	88.4091	27.5814
428	88.4100	27.5766
429	88.3961	27.5841
430	88.3941	27.5826
431	88.3964	27.5823
432	88.4267	27.5752

Sl. No	X_Long	Y_Lat
433	88.4252	27.5741
434	88.4288	27.5765
435	88.4276	27.5665
436	88.4289	27.5638
437	88.4305	27.5635
438	88.4308	27.5647
439	88.4309	27.5635
440	88.4311	27.5640
441	88.4260	27.5552
442	88.4264	27.5559
443	88.4279	27.5570
444	88.4269	27.5539
445	88.4252	27.5537
446	88.4255	27.5526
447	88.4260	27.5493
448	88.4212	27.5570
449	88.4218	27.5598
450	88.4206	27.5555
451	88.4147	27.5611
452	88.4074	27.5591
453	88.4059	27.5572
454	88.4097	27.5490
455	88.3972	27.5431
456	88.3966	27.5535
457	88.3909	27.5492
458	88.3798	27.5522
459	88.3799	27.5511
460	88.3816	27.5506
461	88.3819	27.5510
462	88.3858	27.5597
463	88.3818	27.5478
464	88.3646	27.5569
465	88.3583	27.5534
466	88.3431	27.5625
467	88.3408	27.5607
468	88.3607	27.5844
469	88.3612	27.5803
470	88.3523	27.5832
471	88.3476	27.5874
472	88.3507	27.5869
473	88.2878	27.5398
474	88.2880	27.5404
475	88.2877	27.5418
476	88.2879	27.5414

Sl. No	X_Long	Y_Lat
477	88.2877	27.5653
478	88.2856	27.5620
479	88.3036	27.6389
480	88.3139	27.6536
481	88.3165	27.6500
482	88.3173	27.6500
483	88.3215	27.6460
484	88.3180	27.6336
485	88.3089	27.6317
486	88.3115	27.6321
487	88.3120	27.6320
488	88.3121	27.6324
489	88.3250	27.6373
490	88.3311	27.6310
491	88.3302	27.6325
492	88.3292	27.6354
493	88.3267	27.6283
494	88.3379	27.6135
495	88.3465	27.6196
496	88.3797	27.6246
497	88.3798	27.6259
498	88.3739	27.6172
499	88.3713	27.6157
500	88.3562	27.6120
501	88.3540	27.5956
502	88.3520	27.6015
503	88.3557	27.6056
504	88.3532	27.6060
505	88.3679	27.5951
506	88.3680	27.5661
507	88.3617	27.5612
508	88.3695	27.5696
509	88.3930	27.5859
510	88.4304	27.5856
511	88.4264	27.5851
512	88.4316	27.5834
513	88.4356	27.5878
514	88.4376	27.5902
515	88.4389	27.5932
516	88.4400	27.5953
517	88.4353	27.6002
518	88.4351	27.5989
519	88.4267	27.6030
520	88.4296	27.6000

Sl. No	X_Long	Y_Lat
521	88.4263	27.5960
522	88.4259	27.5930
523	88.4290	27.6099
524	88.4318	27.6107
525	88.4367	27.6111
526	88.4355	27.6088
527	88.4274	27.6069
528	88.4495	27.6078
529	88.4483	27.6049
530	88.4562	27.6106
531	88.4604	27.6082
532	88.4539	27.6206
533	88.4534	27.6203
534	88.4486	27.6241
535	88.4505	27.6250
536	88.4513	27.6246
537	88.4424	27.6202
538	88.4439	27.6083
539	88.4450	27.6096
540	88.4437	27.6050
541	88.4422	27.6036
542	88.4419	27.5974
543	88.4402	27.5975
544	88.4453	27.6030
545	88.4460	27.6192
546	88.4558	27.6276
547	88.4608	27.6235
548	88.4529	27.6339
549	88.4541	27.6385
550	88.4433	27.6411
551	88.4477	27.6498
552	88.4486	27.6508
553	88.4381	27.6748
554	88.4607	27.6588
555	88.4705	27.6287
556	88.4444	27.6497
557	88.4490	27.6378
558	88.4560	27.6093
559	88.4530	27.6082
560	88.4571	27.6047
561	88.4571	27.6056
562	88.4573	27.5958
563	88.4632	27.5984
564	88.4633	27.6001

Sl. No	X_Long	Y_Lat
565	88.4623	27.5985
566	88.4619	27.5840
567	88.4538	27.5829
568	88.4523	27.5824
569	88.4532	27.5819
570	88.4601	27.5852
571	88.4521	27.5942
572	88.4428	27.5645
573	88.4453	27.5658
574	88.4363	27.5624
575	88.4371	27.5621
576	88.4392	27.5599
577	88.4408	27.5596
578	88.4392	27.5588
579	88.4530	27.5701
580	88.4568	27.5740
581	88.4599	27.5736
582	88.4672	27.5752
583	88.4597	27.5675
584	88.4115	27.5192
585	88.4739	27.6127
586	88.4755	27.6127
587	88.4771	27.6129
588	88.4776	27.6134
589	88.4819	27.6029
590	88.4831	27.6108
591	88.4080	27.5149
592	88.4104	27.5168
593	88.4096	27.5156
594	88.4107	27.5161
595	88.4112	27.5167
596	88.4108	27.5184
597	88.4120	27.5169
598	88.4042	27.5080
599	88.4046	27.5092
600	88.3992	27.5057
601	88.4003	27.5069
602	88.3991	27.5022
603	88.4005	27.5037
604	88.3943	27.5027
605	88.3932	27.5125
606	88.3876	27.4745
607	88.3861	27.4689
608	88.3865	27.4714

Sl. No	X_Long	Y_Lat
609	88.3885	27.4707
610	88.3865	27.4646
611	88.3878	27.4664
612	88.3777	27.4672
613	88.3642	27.4638
614	88.3498	27.4505
615	88.3301	27.4948
616	88.3260	27.4863
617	88.3213	27.4801
618	88.3181	27.4745
619	88.3171	27.4779
620	88.3272	27.4221
621	88.3405	27.4339
622	88.3367	27.4406
623	88.3395	27.4450
624	88.3299	27.3858
625	88.3268	27.3866
626	88.3269	27.3883
627	88.3319	27.3900
628	88.3344	27.3895
629	88.3392	27.3867
630	88.3399	27.3891
631	88.3395	27.3902
632	88.3305	27.3893
633	88.3273	27.3884
634	88.3430	27.3722
635	88.3480	27.3774
636	88.3486	27.3772
637	88.3546	27.3787
638	88.3224	27.3630
639	88.3216	27.3613
640	88.3136	27.3111
641	88.3158	27.3126
642	88.3146	27.3128
643	88.3141	27.3118
644	88.3107	27.3110
645	88.3064	27.3038
646	88.3146	27.3022
647	88.3159	27.3035
648	88.3191	27.3022
649	88.3229	27.3129
650	88.3215	27.3125
651	88.3269	27.3150
652	88.3311	27.3148

Sl. No	X_Long	Y_Lat
653	88.3306	27.3150
654	88.3330	27.3204
655	88.4326	27.3381
656	88.4308	27.3297
657	88.4206	27.3278
658	88.4179	27.3313
659	88.4167	27.3297
660	88.4286	27.3541
661	88.3993	27.3231
662	88.4021	27.3240
663	88.4277	27.3188
664	88.3938	27.3040
665	88.3970	27.2993
666	88.4036	27.2999
667	88.3029	27.3209
668	88.3008	27.3214
669	88.2939	27.3271
670	88.2918	27.3358
671	88.2958	27.3410
672	88.3046	27.3431
673	88.3087	27.3420
674	88.2745	27.3354
675	88.2626	27.3384
676	88.2170	27.3859
677	88.2201	27.3857
678	88.2119	27.3898
679	88.2105	27.3913
680	88.2128	27.3914
681	88.2067	27.3932
682	88.2086	27.3899
683	88.2044	27.3843
684	88.2070	27.3846
685	88.1989	27.3764
686	88.2026	27.3757
687	88.2136	27.4018
688	88.1911	27.4162
689	88.1924	27.4152
690	88.1929	27.4147
691	88.1965	27.4202
692	88.2075	27.4217
693	88.1994	27.4130
694	88.1996	27.4063
695	88.1822	27.4671
696	88.1847	27.4667

Sl. No	X_Long	Y_Lat
697	88.1922	27.4676
698	88.1884	27.4656
699	88.1881	27.4654
700	88.1855	27.4438
701	88.2222	27.4403
702	88.2246	27.4428
703	88.2270	27.4471
704	88.2267	27.4461
705	88.2532	27.4572
706	88.2558	27.4526
707	88.2462	27.4421
708	88.2651	27.4445
709	88.2604	27.4413
710	88.2617	27.4445
711	88.2671	27.4295
712	88.2675	27.4285
713	88.2645	27.4315
714	88.2673	27.4356
715	88.2677	27.4337
716	88.2532	27.4726
717	88.2538	27.4637
718	88.2627	27.4587
719	88.2548	27.4586
720	88.2633	27.4644
721	88.2636	27.4673
722	88.2653	27.4849
723	88.2623	27.4841
724	88.2626	27.4809
725	88.3040	27.3997
726	88.3088	27.3972
727	88.2978	27.4270
728	88.2976	27.4381
729	88.3042	27.4444
730	88.1884	27.3842
731	88.1936	27.3867
732	88.1787	27.3708
733	88.1758	27.3676
734	88.1610	27.3685
735	88.1826	27.4448
736	88.2850	27.3722
737	88.2932	27.3643
738	88.3108	27.3683
739	88.3095	27.3393
740	88.3138	27.3438
741	88.1760	27.3265
742	88.1660	27.3254
743	88.1871	27.3185
744	88.1474	27.3317
745	88.1437	27.3054
746	88.1449	27.3061
747	88.2217	27.2969
748	88.2181	27.2912
749	88.2145	27.2881
750	88.2285	27.2969
751	88.2470	27.2996
752	88.2645	27.2936
753	88.2656	27.2904
754	88.2668	27.2913
755	88.2642	27.2877
756	88.2650	27.2868
757	88.2812	27.2928
758	88.2817	27.2958
759	88.2858	27.2923
760	88.2756	27.2901
761	88.2713	27.3031
762	88.2718	27.3034
763	88.2801	27.3080
764	88.2706	27.3306
765	88.2702	27.3290
766	88.2687	27.3300
767	88.2649	27.3299
768	88.1824	27.3654
769	88.3767	27.1520
770	88.3771	27.1523
771	88.3811	27.1525
772	88.3821	27.1521
773	88.3710	27.1573
774	88.3359	27.1471
775	88.3358	27.1487
776	88.3390	27.1478
777	88.3388	27.1493
778	88.3332	27.1457
779	88.3307	27.1446
780	88.3255	27.1412
781	88.3205	27.1382
782	88.3212	27.1390
783	88.3194	27.1334
784	88.3209	27.1287

Sl. No	X_Long	Y_Lat
785	88.3191	27.1274
786	88.3165	27.1281
787	88.3170	27.1292
788	88.3171	27.1288
789	88.3124	27.1308
790	88.3114	27.1282
791	88.2927	27.1294
792	88.2943	27.1291
793	88.2950	27.1333
794	88.2986	27.1311
795	88.2983	27.1332
796	88.2701	27.1162
797	88.2715	27.1166
798	88.2663	27.1154
799	88.2674	27.1152
800	88.2668	27.1147
801	88.2646	27.1140
802	88.2651	27.1165
803	88.2646	27.1166
804	88.2644	27.1169
805	88.2754	27.1153
806	88.2808	27.1199
807	88.2812	27.1203
808	88.2577	27.1135
809	88.2583	27.1136
810	88.2589	27.1140
811	88.2617	27.1158
812	88.2561	27.1156
813	88.2557	27.1150
814	88.2562	27.1150
815	88.2540	27.1138
816	88.2547	27.1141
817	88.2556	27.1161
818	88.2565	27.1139
819	88.2417	27.1072
820	88.2426	27.1120
821	88.2417	27.1121
822	88.2446	27.1123
823	88.2420	27.1106
824	88.2332	27.1047
825	88.2500	27.1095
826	88.2220	27.0867
827	88.2238	27.0884
828	88.2251	27.0880

Sl. No	X_Long	Y_Lat
829	88.2201	27.0932
830	88.2662	27.1303
831	88.2678	27.1314
832	88.2632	27.1322
833	88.2608	27.1309
834	88.2617	27.1305
835	88.2611	27.1301
836	88.2645	27.1310
837	88.2645	27.1323
838	88.2655	27.1292
839	88.2661	27.1298
840	88.2493	27.1300
841	88.2497	27.1304
842	88.2499	27.1283
843	88.2492	27.1286
844	88.2513	27.1294
845	88.2514	27.1309
846	88.2548	27.1287
847	88.2550	27.1280
848	88.2551	27.1289
849	88.2506	27.1353
850	88.2512	27.1339
851	88.2520	27.1331
852	88.2520	27.1322
853	88.2530	27.1308
854	88.2439	27.1300
855	88.2435	27.1329
856	88.2438	27.1331
857	88.2430	27.1329
858	88.2425	27.1329
859	88.2438	27.1293
860	88.2440	27.1287
861	88.2450	27.1233
862	88.2449	27.1240
863	88.2431	27.1252
864	88.2450	27.1328
865	88.2492	27.1328
866	88.2462	27.1295
867	88.2340	27.1214
868	88.2354	27.1208
869	88.2367	27.1217
870	88.2361	27.1230
871	88.2371	27.1232
872	88.2389	27.1224

Sl. No	X_Long	Y_Lat
873	88.2399	27.1220
874	88.2224	27.1157
875	88.2226	27.1148
876	88.2224	27.1137
877	88.2226	27.1134
878	88.2236	27.1157
879	88.2097	27.1164
880	88.2098	27.1159
881	88.2110	27.1147
882	88.2107	27.1154
883	88.2113	27.1171
884	88.2103	27.1174
885	88.2098	27.1144
886	88.2102	27.1151
887	88.2138	27.1158
888	88.2144	27.1195
889	88.2143	27.1192
890	88.2145	27.1176
891	88.2154	27.1116
892	88.2289	27.0908
893	88.2279	27.0896
894	88.2348	27.1028
895	88.2358	27.1052
896	88.2350	27.1053
897	88.2351	27.1030
898	88.2357	27.1027
899	88.2497	27.1119
900	88.2348	27.1208
901	88.2357	27.1212
902	88.2370	27.1217
903	88.2372	27.1221
904	88.2345	27.1289
905	88.2345	27.1269
906	88.2261	27.1248
907	88.2276	27.1243
908	88.2277	27.1240
909	88.2963	27.1801
910	88.3028	27.1916
911	88.3159	27.2230
912	88.3152	27.2210
913	88.3148	27.2220
914	88.3141	27.2202
915	88.3136	27.2211
916	88.3161	27.2177

Sl. No	X_Long	Y_Lat
917	88.3178	27.2171
918	88.3102	27.2240
919	88.3102	27.2235
920	88.3115	27.2209
921	88.3158	27.2234
922	88.3130	27.2273
923	88.3128	27.2275
924	88.3117	27.2274
925	88.3215	27.2315
926	88.3216	27.2309
927	88.3211	27.2271
928	88.3205	27.2271
929	88.3235	27.2321
930	88.3231	27.2309
931	88.3230	27.2319
932	88.3253	27.2271
933	88.3304	27.2307
934	88.3268	27.2251
935	88.3275	27.2255
936	88.3182	27.2232
937	88.3323	27.2273
938	88.3317	27.2281
939	88.3008	27.2383
940	88.3012	27.2378
941	88.3014	27.2379
942	88.3026	27.2345
943	88.3030	27.2353
944	88.3043	27.2369
945	88.3032	27.2363
946	88.3030	27.2362
947	88.3018	27.2366
948	88.3021	27.2359
949	88.3003	27.2331
950	88.2984	27.2408
951	88.2962	27.2412
952	88.2991	27.2415
953	88.2991	27.2418
954	88.2994	27.2421
955	88.3021	27.2363
956	88.3034	27.2359
957	88.2862	27.2453
958	88.2889	27.2429
959	88.2908	27.2421
960	88.3007	27.2505

Sl. No	X_Long	Y_Lat
961	88.3707	27.2155
962	88.3713	27.2158
963	88.3617	27.2049
964	88.3614	27.2072
965	88.3644	27.2047
966	88.3652	27.2062
967	88.3663	27.2071
968	88.3661	27.2080
969	88.3768	27.2261
970	88.3719	27.2247
971	88.3492	27.2230
972	88.3462	27.2171
973	88.2611	27.2717
974	88.2542	27.2701
975	88.2647	27.2784
976	88.2837	27.2746
977	88.2859	27.2758
978	88.1427	27.1651
979	88.1804	27.1429
980	88.1753	27.1336
981	88.1738	27.1323
982	88.1708	27.1294
983	88.1689	27.1263
984	88.1787	27.1338
985	88.1105	27.1252
986	88.1376	27.2411
987	88.1520	27.2693
988	88.1515	27.2673
989	88.1529	27.2661
990	88.1575	27.2676
991	88.1522	27.2685
992	88.1490	27.2697
993	88.1749	27.2726
994	88.1556	27.2831
995	88.2629	27.2898
996	88.2631	27.2905
997	88.2633	27.2904
998	88.2620	27.2895
999	88.2617	27.2890
1000	88.2610	27.2880
1001	88.3035	27.2728
1002	88.3140	27.2680
1003	88.3093	27.2683
1004	88.3093	27.2670

Sl. No	X_Long	Y_Lat
1005	88.3113	27.2643
1006	88.3110	27.2559
1007	88.3311	27.2609
1008	88.3307	27.2608
1009	88.3331	27.2638
1010	88.3346	27.2654
1011	88.3386	27.2627
1012	88.3390	27.2659
1013	88.3355	27.2600
1014	88.3345	27.2594
1015	88.3445	27.2446
1016	88.3819	27.2701
1017	88.3736	27.2682
1018	88.3788	27.2466
1019	88.3887	27.3016
1020	88.3891	27.3020
1021	88.3750	27.3045
1022	88.3755	27.3032
1023	88.2940	27.2455
1024	88.2933	27.2426
1025	88.2617	27.2556
1026	88.2223	27.2255
1027	88.2229	27.2232
1028	88.2090	27.2157
1029	88.2035	27.2213
1030	88.2028	27.2239
1031	88.2005	27.2224
1032	88.2017	27.2231
1033	88.2251	27.2471
1034	88.2362	27.2444
1035	88.2364	27.2258
1036	88.1195	27.2026
1037	88.1276	27.2026
1038	88.6673	27.3082
1039	88.7016	27.2912
1040	88.7035	27.2917
1041	88.7178	27.2932
1042	88.7185	27.2943
1043	88.7190	27.2972
1044	88.7191	27.2987
1045	88.7197	27.2995
1046	88.7193	27.3010
1047	88.7157	27.2984
1048	88.7207	27.3008

Sl. No	X_Long	Y_Lat
1049	88.7229	27.3020
1050	88.7204	27.3044
1051	88.7200	27.3067
1052	88.7241	27.3085
1053	88.7306	27.3174
1054	88.7309	27.3169
1055	88.7277	27.3167
1056	88.7708	27.2975
1057	88.7670	27.2975
1058	88.7627	27.2952
1059	88.6387	27.2138
1060	88.6658	27.2245
1061	88.6465	27.2502
1062	88.6473	27.2500
1063	88.6789	27.2442
1064	88.6903	27.2358
1065	88.7155	27.2840
1066	88.7159	27.2846
1067	88.7497	27.2914
1068	88.7498	27.2916
1069	88.7491	27.2935
1070	88.7505	27.2879
1071	88.7518	27.2881
1072	88.7510	27.2864
1073	88.7511	27.2878
1074	88.7603	27.2959
1075	88.7647	27.2970
1076	88.6158	27.2423
1077	88.6155	27.2786
1078	88.6313	27.2921
1079	88.7230	27.2235
1080	88.7272	27.2212
1081	88.7243	27.2208
1082	88.7543	27.2279
1083	88.7352	27.3141
1084	88.7211	27.3081
1085	88.7214	27.3083
1086	88.7223	27.3090
1087	88.7235	27.3108
1088	88.7308	27.2840
1089	88.7383	27.2829
1090	88.7387	27.2830
1091	88.7743	27.2919
1092	88.8602	27.3134

Sl. No	X_Long	Y_Lat
1093	88.8603	27.3133
1094	88.8381	27.2636
1095	88.8549	27.2691
1096	88.8807	27.3027
1097	88.5770	27.2005
1098	88.5771	27.2004
1099	88.5785	27.2005
1100	88.5876	27.2005
1101	88.5939	27.2003
1102	88.5942	27.2002
1103	88.5943	27.2003
1104	88.7241	27.1972
1105	88.7229	27.1973
1106	88.7221	27.1959
1107	88.5791	27.1858
1108	88.5961	27.1875
1109	88.5964	27.1880
1110	88.6006	27.1902
1111	88.6011	27.1898
1112	88.6023	27.1900
1113	88.6333	27.1954
1114	88.6409	27.1883
1115	88.6404	27.1896
1116	88.6404	27.1899
1117	88.6389	27.1904
1118	88.6386	27.1906
1119	88.6377	27.1897
1120	88.6371	27.1899
1121	88.6403	27.1915
1122	88.6419	27.1918
1123	88.6427	27.1910
1124	88.6031	27.1839
1125	88.7272	27.1551
1126	88.7276	27.1552
1127	88.7236	27.1749
1128	88.6527	27.1637
1129	88.6538	27.1629
1130	88.5491	27.7732
1131	88.5455	27.7745
1132	88.5500	27.7707
1133	88.5496	27.7692
1134	88.5448	27.7735
1135	88.5423	27.7678
1136	88.5310	27.7672

Sl. No	X_Long	Y_Lat
1137	88.5349	27.7686
1138	88.5428	27.7635
1139	88.5498	27.7589
1140	88.5509	27.7591
1141	88.5515	27.7576
1142	88.5475	27.7673
1143	88.5394	27.8565
1144	88.5397	27.8561
1145	88.5310	27.8830
1146	88.5398	27.8864
1147	88.5331	27.9067
1148	88.5215	27.9201
1149	88.5226	27.9374
1150	88.5266	27.9337
1151	88.6282	27.6210
1152	88.6236	27.6210
1153	88.6180	27.6213
1154	88.6250	27.6195
1155	88.6405	27.6123
1156	88.6415	27.6125
1157	88.6593	27.5682
1158	88.6689	27.6021
1159	88.6738	27.6040
1160	88.6801	27.6048
1161	88.5855	27.5471
1162	88.5597	27.5320
1163	88.4302	27.5781
1164	88.7909	27.7563
1165	88.7781	27.7484
1166	88.8122	27.7834
1167	88.8884	27.4959

Sl. No	X_Long	Y_Lat
1168	88.4922	27.5689
1169	88.5395	27.5381
1170	88.3939	27.3038
1171	88.3381	27.3054
1172	88.3344	27.3037
1173	88.5037	27.1535
1174	88.5044	27.1542
1175	88.5053	27.1555
1176	88.5055	27.1564
1177	88.5057	27.1573
1178	88.5061	27.1578
1179	88.5061	27.1582
1180	88.5066	27.1574
1181	88.5123	27.1524
1182	88.5033	27.1524
1183	88.4885	27.1477
1184	88.4870	27.1474
1185	88.5062	27.1508
1186	88.5048	27.1515
1187	88.5144	27.1510
1188	88.5131	27.1513
1189	88.5113	27.1529
1190	88.4729	27.1373
1191	88.4723	27.1396
1192	88.4761	27.1394
1193	88.4714	27.1409
1194	88.4747	27.1419
1195	88.4758	27.1356
1196	88.4852	27.1369